A UNITED STATES
DEPARTMENT OF
COMMERCE
PUBLICATION

ESSA Technical Memorandum WBTM WR 52

U.S. DEPARTMENT OF COMMERCE
ENVIRONMENTAL SCIENCE SERVICES ADMINISTRATION
Weather Bureau

Sacramento Weather Radar Climatology

R. G. PAPPAS AND C. M. VELIQUETTE

Western Region

SALT LAKE CITY,
UTAH

July, 1970

WESTERN REGION TECHNICAL MEMORANDA

The Technical Memoranda series provide an informal medium for the documentation and quick dissemination of results not appropriate, or not yet ready, for formal publication in the standard journals. The series are used to report on work in progress, to describe technical procedures and practices, or to report to a limited audience. These Technical Memoranda will report on investigations devoted primarily to Regional and local problems of interest mainly to Western Region personnel, and hence will not be widely distributed.

These Memoranda are available from the Western Region Headquarters at the following address: Weather Bureau Western Region Headquarters, Attention SSD, P. O. Box 11188, Federal Building, Salt Lake City, Utah 84111.

The Western Region subseries of ESSA Technical Memoranda, No. 5 (revised edition), No. 10 and all others beginning with No. 24, are available also from the Clearinghouse for Federal Scientific and Technical Information, U. S. Department of Commerce, Sills Building, Port Royal Road, Springfield, Va. 22151. Price: $3.00 paper copy; $0.65 microfiche. Order by accession number shown in parentheses at end of each entry.

Western Region Technical Memoranda:

No. 1* Some Notes on Probability Forecasting. Edward D. Diemer. September 1965.
No. 2 Climatological Precipitation Probabilities. Compiled by Lucianne Miller. December 1965.
No. 3 Western Region Pre- and Post-FP-3 Program. Edward D. Diemer. March 1966.
No. 4 Use of Meteorological Satellite Data. March 1966.
No. 5** Station Descriptions of Local Effects on Synoptic Weather Patterns. Philip Williams. October 1969 (Revised). (PB-178 000)
No. 6 Improvement of Forecast Wording and Format. C. L. Glenn. May 1966.
No. 7 Final Report on Precipitation Probability Test Program. Edward D. Diemer. May 1966.
No. 8 Interpreting the RAREP. Herbert P. Benner. May 1966. (Revised January 1967.)
No. 9 A Collection of Papers Related to the 1966 NMC Primitive-Equation Model. June 1966.
No. 10* Sonic Boom. Loren Crow (6th Weather Wing, USAF, Pamphlet). June 1966. (AD-479 366)
No. 11 Some Electrical Processes in the Atmosphere. J. Latham. June 1966.
No. 12* A Comparison of Fog Incidence at Missoula, Montana, with Surrounding Locations. Richard A. Dightman. August 1966.
No. 13 A Collection of Technical Attachments on the 1966 NMC Primitive-Equation Model. Leonard W. Snellman. August 1966.
No. 14 Applications of Net Radiometer Measurements to Short-Range Fog and Stratus Forecasting at Los Angeles. Frederick Thomas. September 1966.
No. 15 The Use of the Mean as an Estimate of "Normal" Precipitation in an Arid Region. Paul C. Kangieser. November 1966.
No. 16 Some Notes on Acclimatization in Man. Edited by Leonard W. Snellman. November 1966.
No. 17 A Digitalized Summary of Radar Echoes Within 100 Miles of Sacramento, California. J. A. Youngberg and L. B. Overaas. December 1966.
No. 18 Limitations of Selected Meteorological Data. December 1966.
No. 19 A Grid Method for Estimating Precipitation Amounts by Using the WSR-57 Radar. R. Granger. December 1966.
No. 20 Transmitting Radar Echo Locations to Local Fire Control Agencies for Lightning Fire Detection. Robert R. Peterson. March 1967.
No. 21 An Objective Aid for Forecasting the End of East Winds in the Columbia Gorge. D. John Coparanis. April 1967.
No. 22 Derivation of Radar Horizons in Mountainous Terrain. Roger G. Pappas. April 1967.
No. 23 "K" Chart Application to Thunderstorm Forecasts Over the Western United States. Richard E. Hambidge. May 1967.
No. 24 Historical and Climatological Study of Grinnell Glacier, Montana. Richard A. Dightman. July 1967. (PB-178 071)
No. 25 Verification of Operational Probability of Precipitation Forecasts, April 1966 - March 1967. W. W. Dickey. October 1967. (PB-176 240)
No. 26 A Study of Winds in the Lake Mead Recreation Area. R. P. Augulis. January 1968. (PB-177 830)

*Out of Print
**Revised

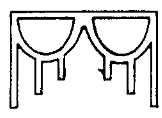

A western Indian symbol for rain. It also symbolizes man's dependence on weather and environment in the West.

U. S. DEPARTMENT OF COMMERCE
ENVIRONMENTAL SCIENCE SERVICES ADMINISTRATION
WEATHER BUREAU

Weather Bureau Technical Memorandum WR- 52

SACRAMENTO WEATHER RADAR CLIMATOLOGY

R. G. Pappas
Weather Bureau Office
Sacramento, California

C. M. Veliquette
Weather Bureau Office
Sacramento, California

WESTERN REGION
TECHNICAL MEMORANDUM NO. 52

SALT LAKE CITY, UTAH
JULY 1970

TABLE OF CONTENTS

		Page
List of Figures		iii
Abstract		1
I.	Introduction	1
II.	Data	2
III.	Limitations	2-4
IV.	Annual, Seasonal, and Monthly Echo Frequency Distributions	5-6
V.	Conclusions	6-7
VI.	References	7

LIST OF FIGURES AND TABLE

		Page
Figure 1(a)	Example of Radar Climatology Computer Output in Map Format	8
Figure 1(b)	Example of Radar Climatology Computer Output in Map Format	9
Figure 2	Average Annual Precipitation (Inches) Map Determined from Radar Integer Data	10
Figure 3	Average Annual Gauge Precipitation During Period of Radar Record	11
Figure 4	Normal Annual Total Precipitation (Inches)--California	12
Figure 5	Average Annual Hourly Echo Frequencies	13
Figure 6	Average "Wet" Season (October-April) Hourly Echo Frequencies	
Figure 7	Average "Wet" Season Gauge Precipitation During Period of Radar Record	15
Figure 8	Average "Dry" Season (May-September) Hourly Echo Frequencies	16
Figure 9	Average "Dry" Season Gauge Precipitation During Period of Radar Record	17
Figure 10	Average January Hourly Echo Frequencies	18
Figure 11	Average February Hourly Echo Frequencies	19
Figure 12	Average March Hourly Echo Frequencies	20
Figure 13	Average April Hourly Echo Frequencies	21
Figure 14	Average May Hourly Echo Frequencies	22
Figure 15	Average June Hourly Echo Frequencies	23
Figure 16	Average July Hourly Echo Frequencies	24
Figure 17	Average August Hourly Echo Frequencies	25
Figure 18	Average September Hourly Echo Frequencies	26
Figure 19	Average October Hourly Echo Frequencies	27
Figure 20	Average November Hourly Echo Frequencies	28
Figure 21	Average December Hourly Echo Frequencies	29
Table 1	Precipitation Stations	4

SACRAMENTO WEATHER RADAR CLIMATOLOGY

ABSTRACT

A climatology of weather radar echoes within 100 nautical miles (n.m.) of Sacramento, California is derived by transferring hourly overlay data onto a coarse grid system. While the program is capable of summarizing rainfall intensities and amounts, limitations in reflectivity--rainfall intensity relationships, particularly for the precipitation climatology of the Sacramento coverage area, severely restrict the utility of such data. However, occurrences of weather echoes, without regard to intensity, do correlate well with normal and observed areal precipitation patterns. The relatively short period of record precludes application of the data in a true climatological sense.

I. INTRODUCTION

An earlier report by Youngberg and Overaas (1966) presented a detailed account of the Sacramento radar climatology program. The Sacramento study and others (e.g., Parrish and Lopez, 1968, or Landers, 1969) have usually summarized only a small amount of data and were aimed primarily at describing techniques and capabilities of the program. Subsequent to the earlier Sacramento report, the available data bank has grown to about seven years of hourly radar data in digitized form, probably one of the longest periods of record for this type of data. Approximately six years (74 months) of the data have now been tabulated, beginning with July 1962 and extending through December 1968, except for the period September-December 1964, when the radar was being moved. Data for 1969 has not yet been processed. A total of 74 months was used in the tabulation.

II. DATA

The earlier work by Youngberg and Overaas (1966) presented a complete explanation of the data base and technique used. In brief: the data base consists of hourly radar overlays which are traced from the Sacramento WSR-57 PPI scope. These overlays include contours of echo intensity in the operational categories specified in the Weather Radar Manual (1967). They are determined from a standard rainfall intensity--reflectivity relationship, $Z_e = 200I^{1.6}$, where Z_e is reflectivity in mm^6/m^3 and I is rainfall in mm/hr. The various intensity levels, very weak, weak, moderate, strong, and very strong, are color coded on the overlay for ease of interpretation. This overlay is an operational tool in the Sacramento radar program, but also serves as an invaluable radar data source, including its use in the climatology study. Intensities within approximately 100 n.m. of the radar are digitized by placing a gridded template over the overlay and coding the intensity for each grid square onto a punch card. The grid is coarse, 64 squares each 22.15 by 22.15 n.m., but allows all intensity data from an overlay to be punched on one card. The gridded template consists of cutout "windows", about one-ninth the area of the squares, in the center of each grid square, and the highest intensity observed in the "window" is the intensity encoded.

The data may then be computer processed in a variety of ways, the most common utilizing a program that prints the hourly frequency of each integer in a map format for any time period desired--day, storm, month, etc. Figures 1(a) and 1(b) are a summary of April data for three years and also an example of the map format. The lowest three intensity integers, 1, 2, and 3, are summed for each grid square in Figure 1(a); while integers 4 and 5 and the totals of 1 through 5 (coded 6) are in Figure 1(b).

III. LIMITATIONS

Limits more restrictive than those usually placed on the reliability of radar data (Battan, 1959; Hiser and Freseman, 1959; Wilson, 1964) must be applied to the Sacramento radar data (Weaver, 1966). Although the antenna is located on top of a tall building, moderately high terrain in the Coast Ranges to the west and high ranges of the Sierra Nevada to the east causes severe blocking over much of the coverage area, in addition to the usual range limitations caused by beam divergence and earth's curvature (Pappas, 1967, 1969). Complete overshooting of precipitation echoes results mostly at ranges more distant than those used in this radar climatology project (i.e., beyond 100 n.m.), but partial blocking combined with strong low level orographic effects causes significant underestimation of intensities during the "wet" season (Pappas, 1969). Convective thunderstorm activity, which occurs almost entirely over the higher ranges of the Sierra Nevada and in Nevada in summer, is detected much more readily due to the high tops attained by these echoes.

Cool, "wet" season storms are characterized by low reflectivities in the upper reaches of the clouds due to the presence of frozen precipitation above the usually low melting levels. Since all the intensity measurements utilize a Z_e - I relationship which is truly applicable to rain only, gross underestimation of precipitation intensities can occur except within about 25 to 75 miles from the radar (Pappas, 1968, 1969). Additional errors are also likely because of the coarse grid size, broad intensity categories, the use of only the small central portion of each grid for representing the entire grid, and the relatively infrequent data samples, i.e., one per hour. Unless taken into account, the variation in drop size distributions is also a critical source of errors when attempting intensity measurements (Stout and Mueller, 1968). Also, minor changes in 1965 in two of the operational intensity categories used by the Weather Bureau cause a slight inconsistency when intensity data prior to the change are combined with later data.

Another shortcoming of the Sacramento radar is the heavy and extensive ground clutter pattern caused by mountains. This often contributes to underestimation of intensities, especially in winter, by requiring the observer to tilt the radar upward several degrees when contouring echoes over mountainous areas. The amount of tilt necessary is usually enough to cause partial, or even complete, overshooting, and can also result in the beam missing low level orographic precipitation or sampling of only the frozen upper portions of storms.

Most of the above effects contribute to gross underestimation of intensities during the cool Pacific storm season--approximately October through April. Attempts are being made to adjust the underestimation for selected hydrologic basins (Pappas, 1969), but no such effort has yet been undertaken for the radar climatology program. This would be very complex and perhaps not feasible because of the large area included in the climatology and the coarse grid and broad intensity categories.

Figure 2 shows average annual radar-determined precipitation based on the entire 74 months of radar data, and Figure 3 is average annual gauge data for 51 stations for the radar period of record.* The 51 stations used are listed by grid location in Table 1. Isohyets based on these data were not drawn due to the poor distribution and relative sparseness of stations used.

---

*Since the radar record is not complete for all years, radar averages and average gauge data for the same period were computed from the monthly averages, i.e., each month's average was determined for either the six or seven years of available data, and these in turn added to obtain the annual (January-December), "wet" season (October-April), and "dry" season (May-September) averages.

TABLE I

PRECIPITATION STATIONS

GRID NO.	STATION	GRID NO.	STATION	GRID NO.	STATION
9	Mineral	29	Grass Valley	50	Petaluma
11	Paskenta	30	Blue Canyon	52	Antioch
14	Greenville	31	Tahoe City	54	San Andreas
15	Quincy	32	Carson City	55	Sonora
16	Doyle	33	Cloverdale	56	Hetch Hetchy
17	Willets	34	Hobergs	58	San Francisco
18	Stonyford	35	Lake Berryessa	59	Oakland
19	Willows	36	Nicolaus	61	Modesto
20	Oroville	37	Auburn	62	Turlock
20	Chico	38	Placerville	64	Yosemite
21	Brush Creek	39	Woodfords	66	Davenport
22	Downieville	41	Fort Ross	67	San Jose
23	Loyalton	42	Santa Rosa	67	Gilroy
24	Reno	43	Napa	69	Newman
25	Ukiah	44	Sacramento	70	Merced
27	Williams	46	Ione	71	Watsonville
28	Yuba City	47	Calaveras R.S.	72	Hollister

Except for grids immediately adjacent to Sacramento, which are remarkably near both climatological normals (Figure 4) and average annual precipitation (Figure 3), radar determined precipitation in Figure 2 appears to underestimate by a factor ranging from less than two to as much as fifteen. In Figure 2, the fact that the northernmost grids are indicated to have considerably more precipitation than those furthest south is realistic, but amounts are still gross underestimates. The overall radar-determined precipitation distribution is one of decreasing amounts with distance in all directions from Sacramento, which is, of course, true only to the southeast over the San Joaquin Valley, and to the northwest over the lower Sacramento Valley.

Although not shown here, the same deficiency is demonstrated in tabulations of the frequency of each integer for the "wet" season. These tabulations show the heavier integers (3, 4, and 5) occurring almost exclusively in the grids nearest to Sacramento. Contributing to this, and also very likely causing some overestimation of intensities near the radar, is the effect of the radar beam sampling the melting layer or bright band at close ranges (Weather Radar Manual, 1967). As would be expected for reasons given above, no such deficiency is indicated for the summer convective season.

Limitations due to the short period of record are significant, particularly for so highly variable a parameter as precipitation. Therefore, applications of the technique must be made with caution and conclusions reached considered as only tentative.

IV. ANNUAL, SEASONAL, AND MONTHLY ECHO FREQUENCY DISTRIBUTIONS

The tabulation of average annual echo frequency for each grid square, without regard to intensities, for all 74 months of data is presented in Figure 5. The 500-echo frequency isopleth in the Coast Range and the 600 isopleth in the Sierra Nevada correspond fairly well with areas of maximum normal (Figure 4) and sample period average (Figure 3) precipitation, with orographic effects playing a major role in the distribution. However, the primary maximum, shown by the 650 isopleth, is shifted southward from its normal or sample period position. This is probably due mostly to the ranging limitations discussed in Section III. The overall decrease in frequencies from north to south is realistic; however, some of the rapid decrease near grid edges is due to range and blocking limitations.

Figure 6 is the echo frequency tabulation for the "wet" season months, October through April. Again, a slight southward shift of the Sierra Nevada maximum is indicated if compared with the averages in Figure 7. The maximum in the Coast Range at grid 34 also corresponds with maximum in Figure 7. However, high values shown in grids 33 and 17 of Figure 7 are not indicated in the radar analysis, Figure 6, probably due to range limitations. The rapid decrease in echo frequencies in the lee of the Sierra is due mostly to the normal lee rain-shadow effect and agrees well with the gauge averages (Figures 4 and 7). This decrease also results to some degree from range limitations and blocking.

"Dry" season (May through September) totals are presented in Figure 8. In this case, echo maximum areas enclosed by the 90 isopleths are in two different portions of the Sierra Nevada. These compare favorably with gauge averages in Figure 9, which indicate maxima in grids 30 and 56 (unfortunately, no gauge data were computed for grid 48). The minimum in the northern Sierra at grid 14 (60 isopleth in Figure 8) reflects a minimum gauge precipitation area in the same grid in Figure 9. More about the "dry" season distributions will be included in the discussion of monthly averages.

Monthly frequency averages are presented in Figures 10 through 21. Generally, the rapid decrease in echo frequency between the "wet" and "dry" seasons is indicated by comparing April (Figure 13) and May (Figure 14). The reverse transition from October (Figure 19) to November (Figure 20) is also very pronounced.

Beginning in May, an eastward to southeastward shift in echo frequency maximum occurs. In May, the evidence is only a submaximum (30 isopleth) in grid 48. By July the maximum has shifted east of the Sierra Nevada crest and continues there through September. This shift is attributed to the waning influence of westerly disturbances during summer months and the increasing effect of moist unstable air masses penetrating the coverage area from the southeast, with orographic lifting and surface heating helping to trigger further instability. Additionally, nondetection of much of the distant cool, "wet" season precipitation contrasted with enhanced summertime detection capability, as discussed in section

III, probably influences the magnitude of this shift. An earlier study by Benner, et al, (1962) showed a similar echo maximum in summer in the approximate area of grid 48. Submaxima are indicated in August in the Coast Range (grid 34) and the north end of the Sacramento Valley (grid 12). The diurnal characteristics of this convective activity is well known, and a radar view of this is also discussed thoroughly by Benner, et al, (1962).

By October, storms moving from the Pacific become more frequent, causing the return of the echo maximum to the west slopes of the Sierra Nevada. The "wet" season months (October through April) are all characterized by an echo frequency maximum on the Sierra Nevada west slopes and a submaximum in the Coast Range. This again indicates the overwhelming role played by orographic lifting in producing more persistent as well as heavier precipitation over mountain regions. Normal precipitation in the coverage area is characterized by rapidly increasing monthly amounts from the end of the summer until December or January, then a gradual decrease into spring months. However, radar echo frequencies indicate less occurrences in December than November and again less occurrences in February than March and April. This can be explained by probable short term influences during the radar period of record which began in 1962. Decembers have had below normal precipitation in Sacramento in all years since 1962, except the very wet one in 1964, which is not included in the radar averages because the radar set was being moved to a new location at that time. Also, most Novembers during the radar data period have had above normal precipitation. The radar anomaly in February is matched by the Sacramento gauge record which shows significantly below normal February precipitation from 1963 to 1968. March and April Sacramento gauge data have both shown near or above normal precipitation during the radar data period, with two very wet years for both months, 1963 and 1967, probably accounting for much of the high average radar frequencies.

V. CONCLUSIONS

Employing a simple operational data base, a radar climatology of echoes within 100 n.m. of Sacramento has been developed for approximately six years of data. Despite inherent radar limitations and the coarse grid system, many significant features of the rainfall climatology of the area may be discerned. However, the relatively short period of present radar records reduces their significance for most applications.

Further application of the radar data, including additional use of intensity statistics, can be made by linking the data to other meteorological parameters. These could include studies in synoptic climatology, short range precipitation forecasting, and hydrology. One project which would not rely heavily on correlation with established climatological data concerns determination of an independent summertime convective rainfall frequency climatology. The density of rainfall gauges and reporting stations in remote mountain areas is probably far from adequate considering the localized nature of this convective activity. Radar determination of summertime convective intensity is much more feasible than for winter season precipitation because most restrictions mentioned in section III, are not significant for summer rainfall. However, other limitations, e.g., the presence of hail and virga causing overestimation of rainfall, short period records, and coarse grid size would have to be considered.

VI. REFERENCES

Battan, L. J., Radar Meteorology, The University of Chicago Press, 1959, 161 pp.

Benner, H. B., et al, "Summer Convective Cell Radar Patterns Over Northern and Central California," Monthly Weather Review, Volume 90, No. 10, October 1962, pp. 425-430.

Hiser, H. W., and Freseman, W. L., Radar Meteorology, The Marine Laboratory, University of Miami, Coral Gables, Florida, 1959, 267 pp.

Landers, H., "South Carolina Radar Climatology April-November 1968," Climatic Research Series No. 6, Clemson University Agricultural Experiment Station in Cooperation with U. S. Department of Commerce, ESSA, Weather Bureau, October 1969, 8 pp.

Pappas, R. G., "Derivation of Radar Horizons in Mountainous Terrain," Western Region Technical Memorandum No. 22, April 1967, 6 pp.

Pappas, R. G., "Melting Level and Topographic Influences on Weather Radar's Effectiveness," unpublished report, January 1968, 6 pp.

Pappas, R. G., "Radar Assessment of Areal Precipitation Over Northern California," unpublished report, March 1969, 7 pp.

Parrish, S. K., and Lopez, M. A., "A Study of the Areal Distribution of Radar Detected Precipitation at Charleston, South Carolina," ESSA Technical Memorandum WBTM-ER-31, October 1968, 4 pp.

Stout, G. E., and Mueller, E. A., "Survey of Relationships Between Rainfall Rate and Radar Reflectivity in the Measurement of Precipitation," Journal of Applied Meteorology, Volume 7, No. 3, June 1968, pp. 465-474.

Weather Radar Manual, WBAN, Washington, D. C., August 1967, Part B, p. 5-5.

Weaver, R. L., "California Storms as Viewed by Sacramento Radar," Monthly Weather Review, Volume 94, No. 7, July 1966, pp. 466-474.

Wilson, J. W., "Evaluation of Precipitation Measurements with the WSR-57 Weather Radar," Journal of Applied Meteorology, Volume 3, No. 2, April 1964, pp. 164-174.

Youngberg, J. A., and Overaas, L. B., "A Digitalized Summary of Radar Echoes Within 100 Miles of Sacramento," Western Region Technical Memorandum No. 17, December 1966, 10 pp.

INTENSITY LEVEL								
1				14	4			
2				270	189			
3				6	0			
1		4	16	9	1	1	0	
2		158	213	304	260	192	41	
3		1	9	21	3	2	0	
1	7	5	15	11	4	2	0	0
2	138	147	228	288	348	268	73	14
3	1	2	14	38	27	3	0	0
1	20	16	12	3	3	2	3	0
2	184	201	199	224	307	344	247	40
3	1	9	20	33	34	22	1	0
1	22	21	11	7	4	3	1	0
2	148	271	185	243	339	390	255	95
3	0	17	29	37	45	35	5	0
1	26	23	16	4	2	3	1	1
2	154	215	231	210	290	345	303	211
3	1	11	34	43	46	39	7	3
1	22	25	17	5	2	6	4	4
2	99	218	222	188	245	274	293	263
3	2	14	49	35	47	33	13	4
1	19	17	13	5	1	3	1	1
2	125	176	215	165	224	256	255	223
3	2	5	18	18	14	22	14	3
1		10	6	4	1	1	3	
2		135	185	181	192	192	188	
3		3	3	7	6	3	3	
1				1	0			
2				83	103			
3				1	0			

FIGURE 1(a). Example of Radar Climatology Computer Output in Map Format. April 1963, 1964, 1965 for Intensity Levels 1, 2, and 3.

INTENSITY LEVEL								
4				2	0			
5				0	0			
6				292	193			
4		1	3	3	0	0	0	
5		0	0	0	0			
6		164	241	337	264	195	41	
4	0	0	2	6	1	0	0	0
5	0	0	0	0				
6	146	154	259	343	380	273	73	14
4	0	0	3	11	5	2	0	0
5	0	0	0	0				
6	205	226	234	271	349	370	251	40
4	1	0	2	9	6	5	0	0
5	0	0	0	0				
6	171	309	227	296	394	433	261	95
4	0	1	0	6	2	3	0	0
5	0	0	0	0				
6	181	250	281	263	340	390	311	215
4	0	0	1	1	5	6	1	0
5	0	1	0	0	0	0		0
6	123	258	289	229	299	319	311	271
4	0	0	0	0	0	1	0	0
5	0	0	0	0				
6	146	198	246	188	239	282	270	227
4		0	0	0				
5		0	0	0				
6		148	194	192	199	196	194	
4				0	0			
5				0	0			
6				85	103			

FIGURE 1(b). Example of Radar Climatology Computer Output in Map Format. April 1963, 1964, 1965 for Intensity Levels 4 and 5 and Totals of 1 through 5 (coded 6).

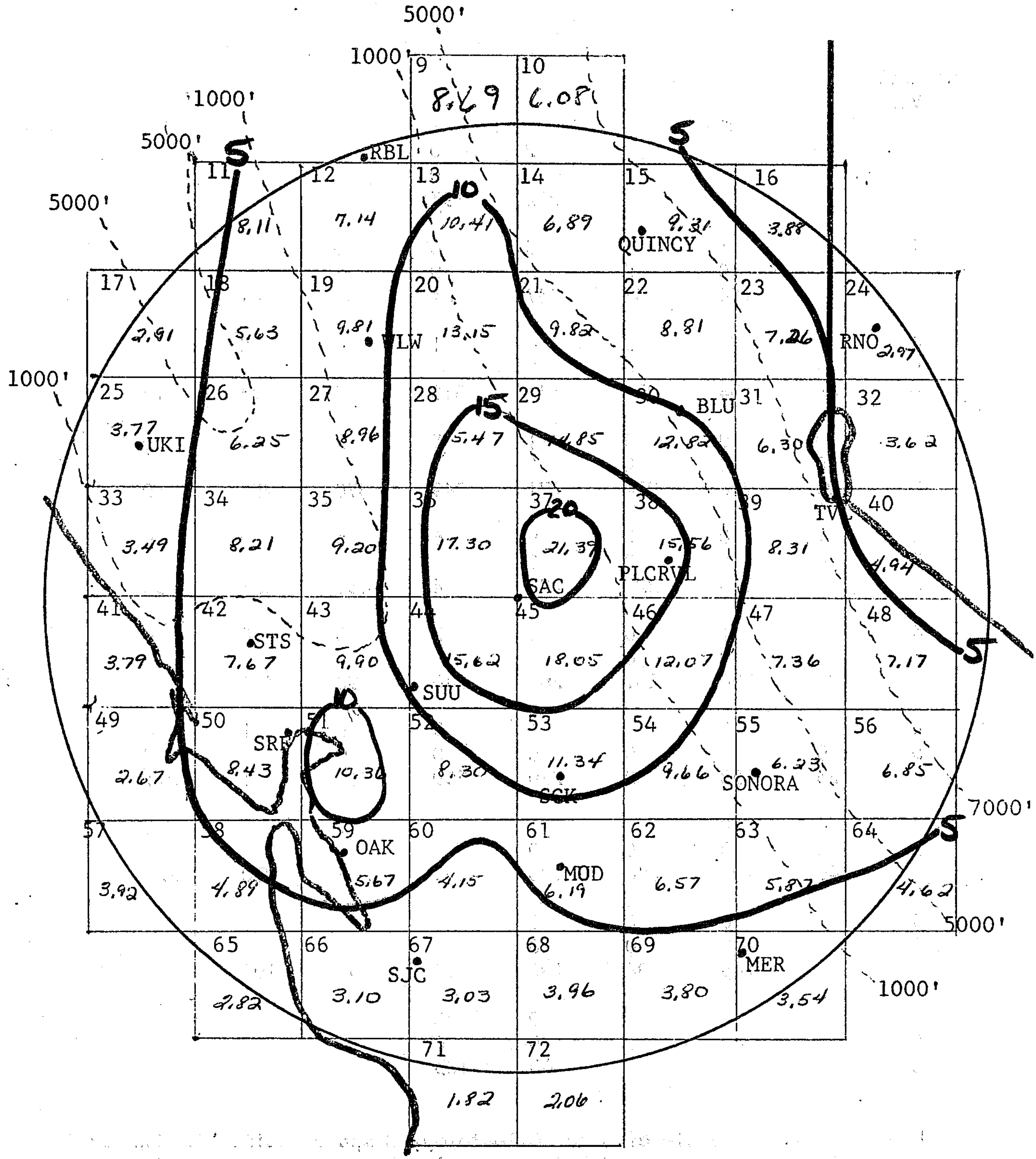

FIGURE 2. Average annual precipitation (inches) map determined from radar integer data. Dashed lines are approximate terrain contours. Grid numbers are in upper left corner of each square. Range circle is at 100 nautical miles.

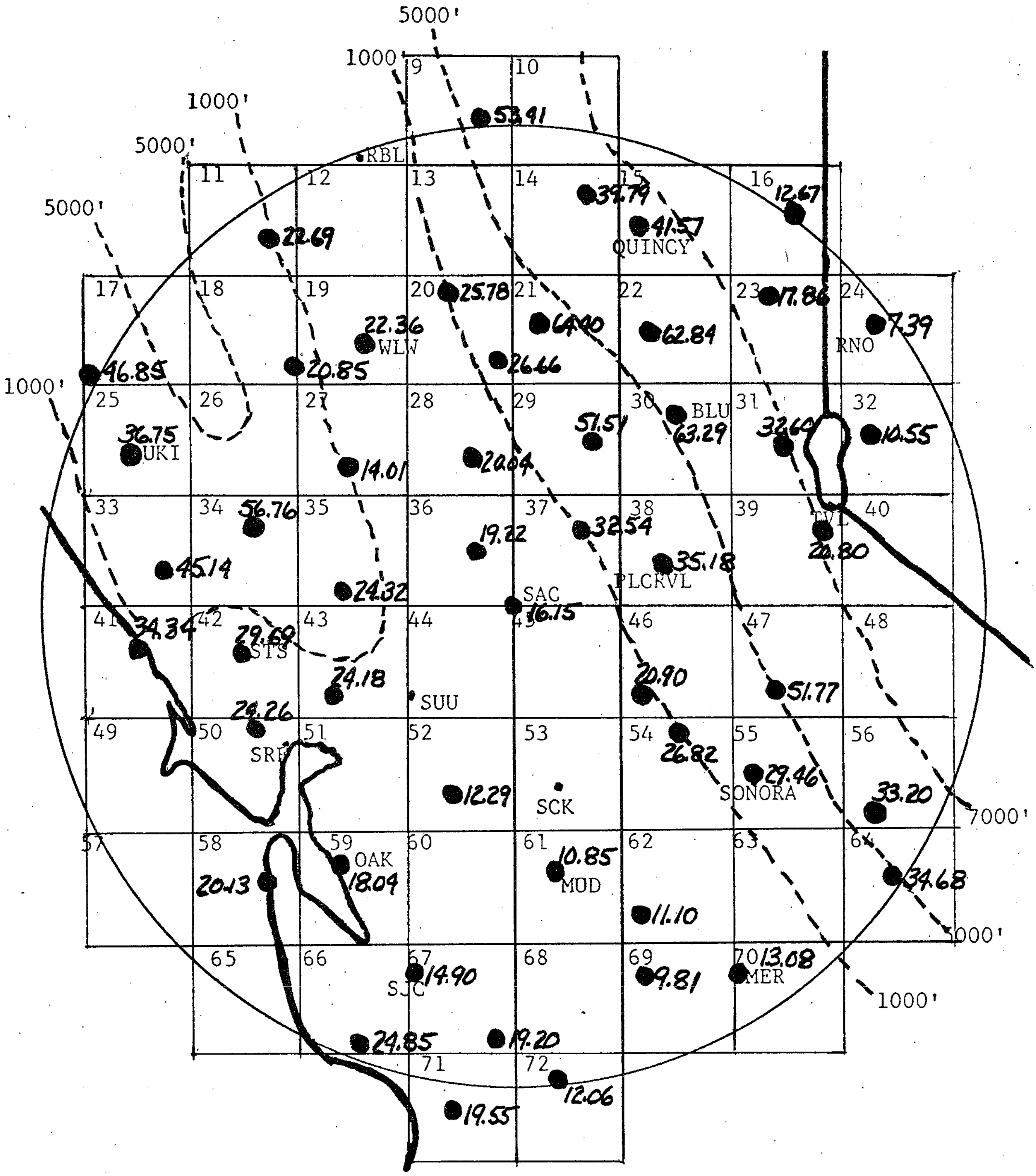

FIGURE 3. Average annual gauge precipitation during period of radar record. See Table I in text for list of stations used. Legend as in Figure 2.

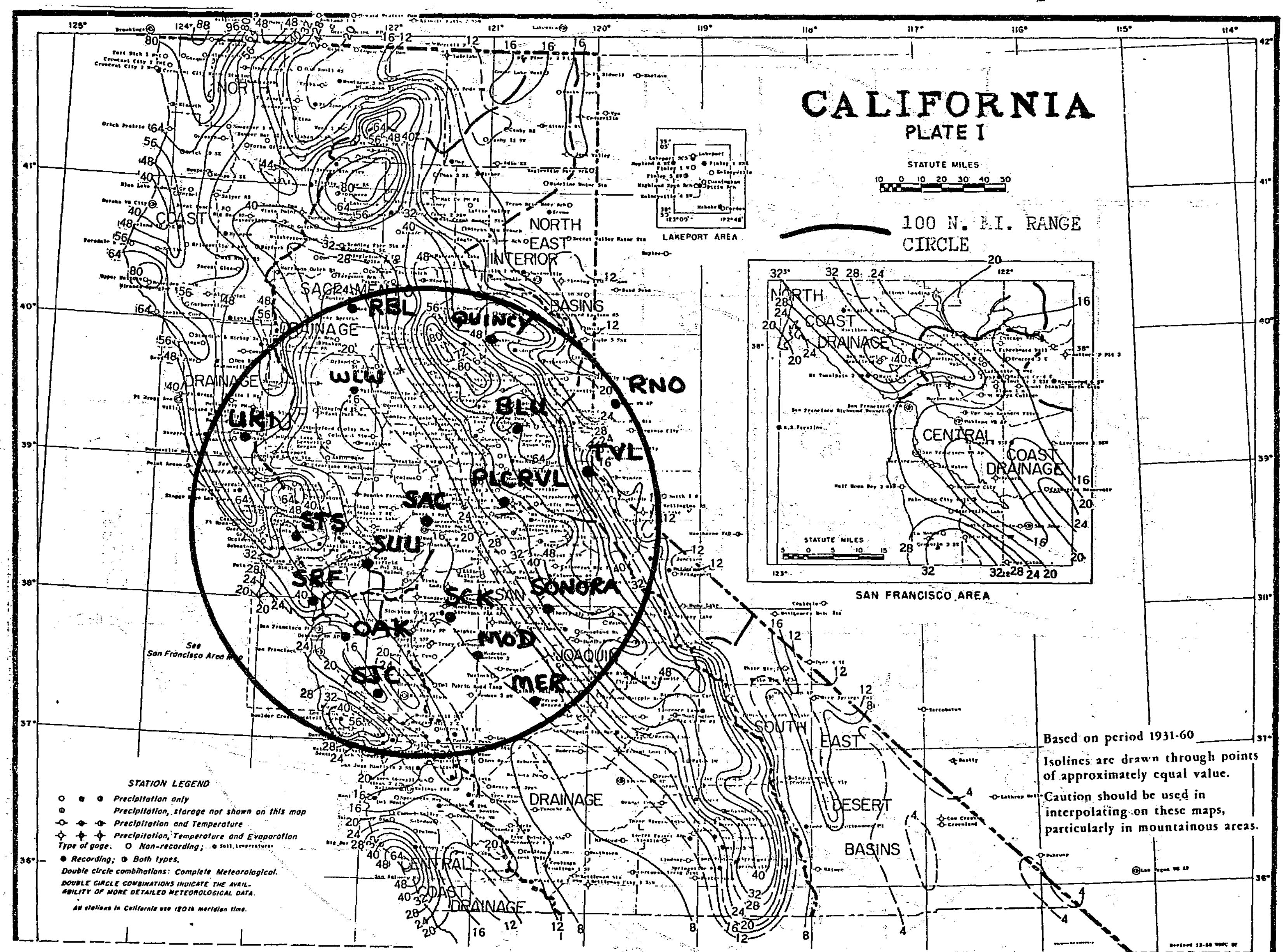

FIGURE 4. Normal Annual Total Precipitation (Inches)--California.

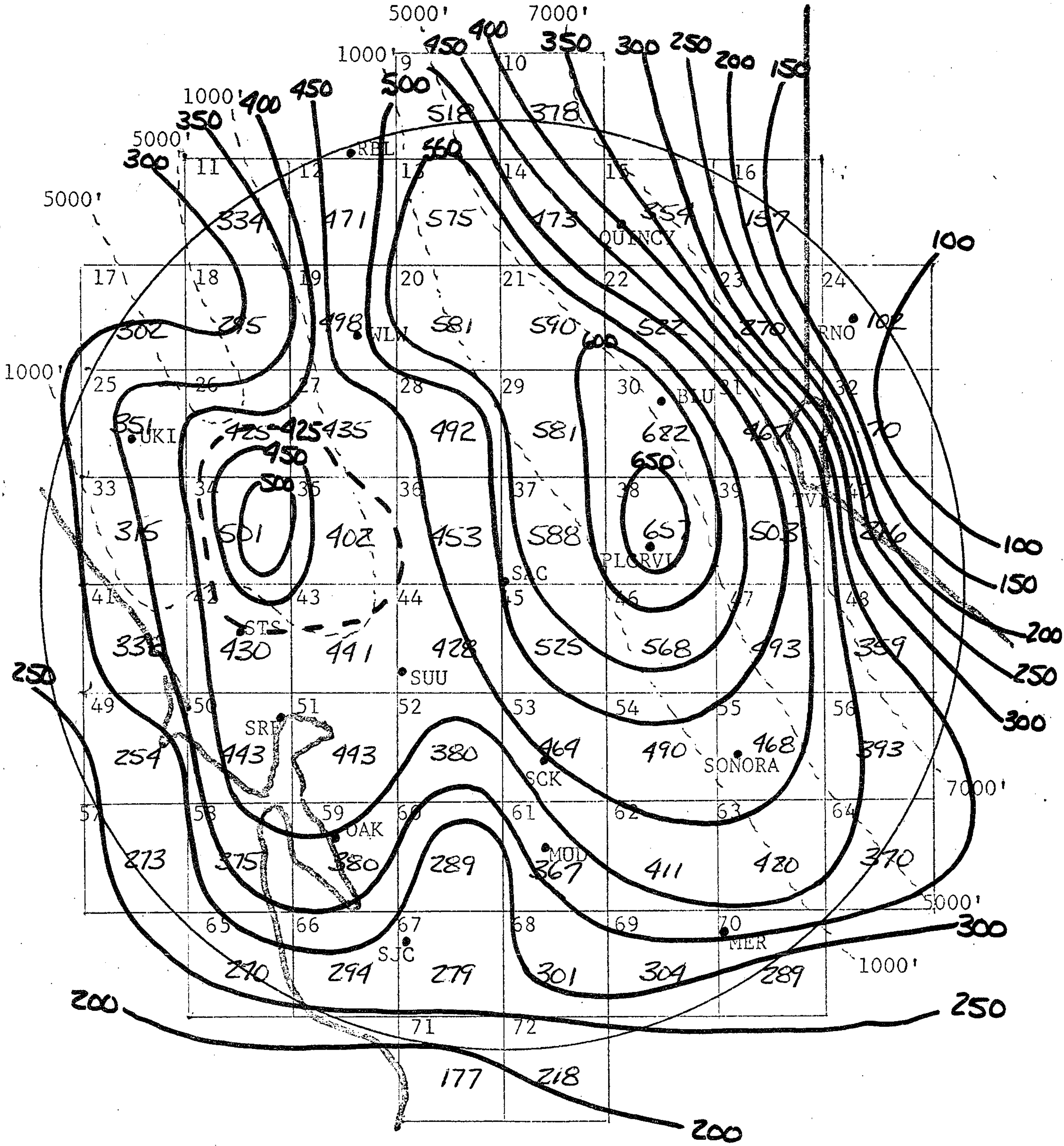

FIGURE 5. Average annual hourly echo frequencies. Dashed lines are approximate terrain contours. Grid numbers are in upper left corner of each square. Range circle is at 100 n.m.

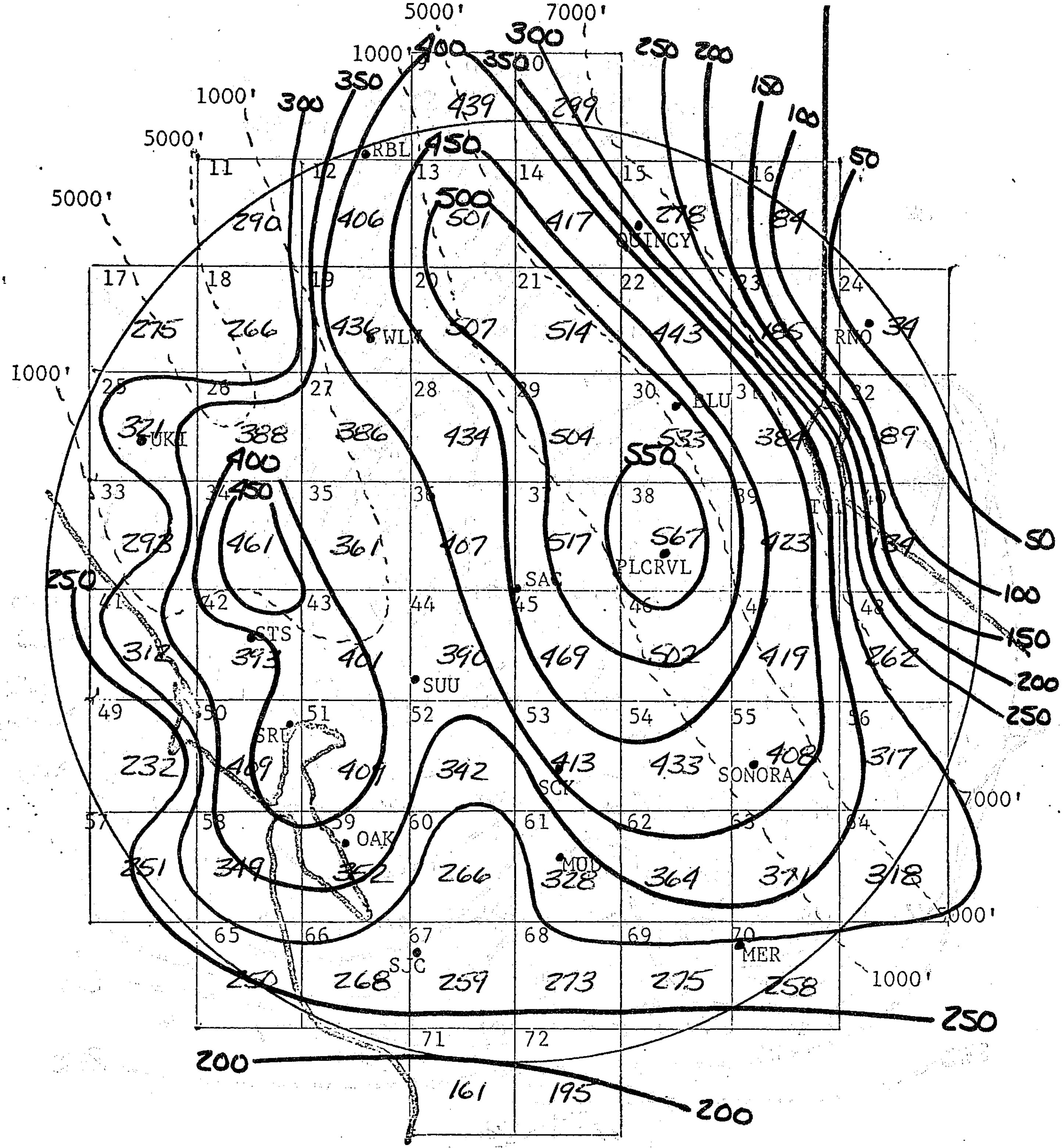

FIGURE 6. Average "wet" season (October-April) hourly echo frequencies. Dashed lines are approximate terrain contours. Grid numbers are in upper left corner of each square. Range circle is at 100 nautical miles.

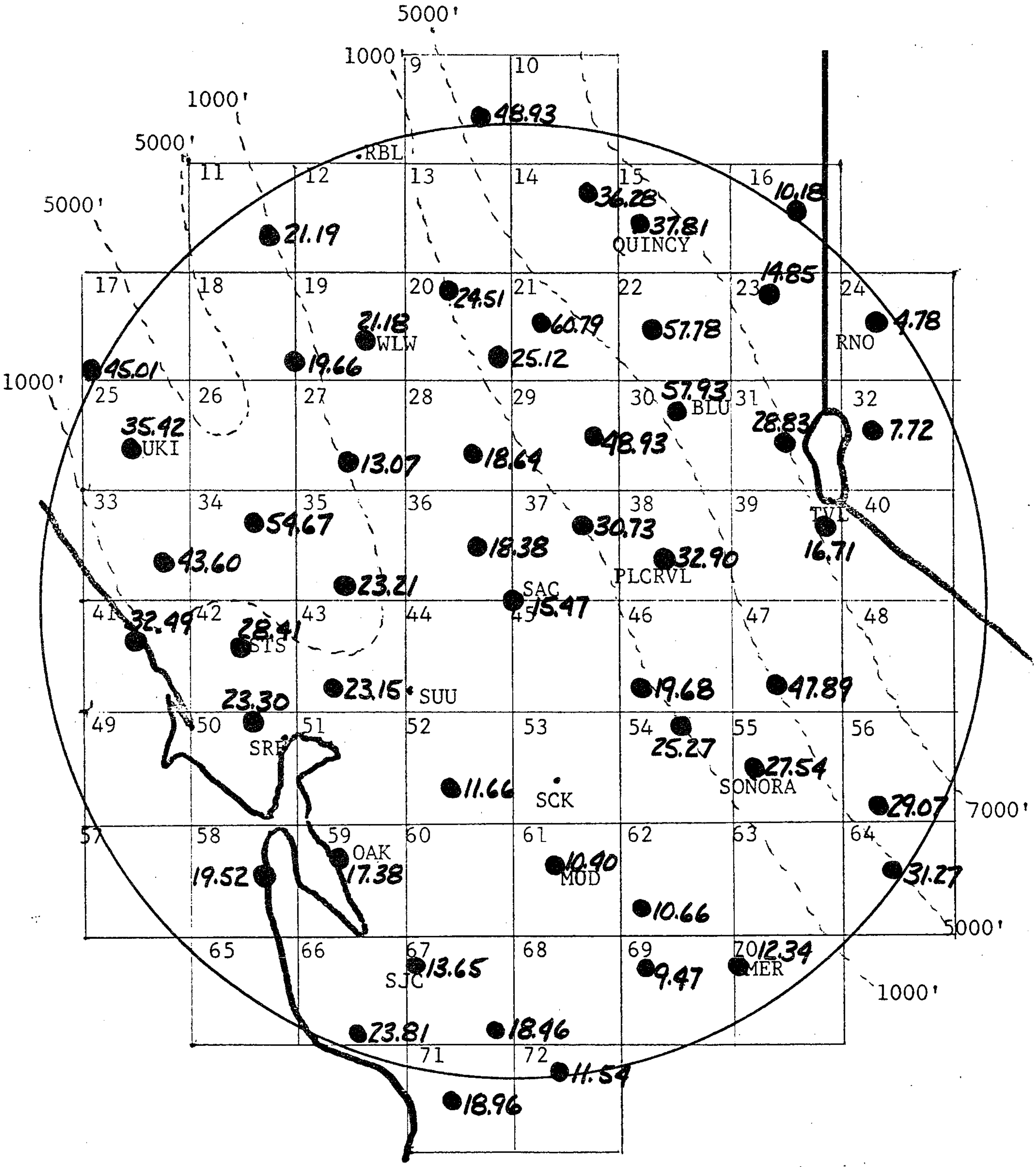

FIGURE 7. Average "wet" season gauge precipitation during period of radar record. See Table 1 in text for list of stations used. Dashed lines are approximate terrain contours. Grid numbers are in upper left corner of each square. Range circle is at 100 n.m.

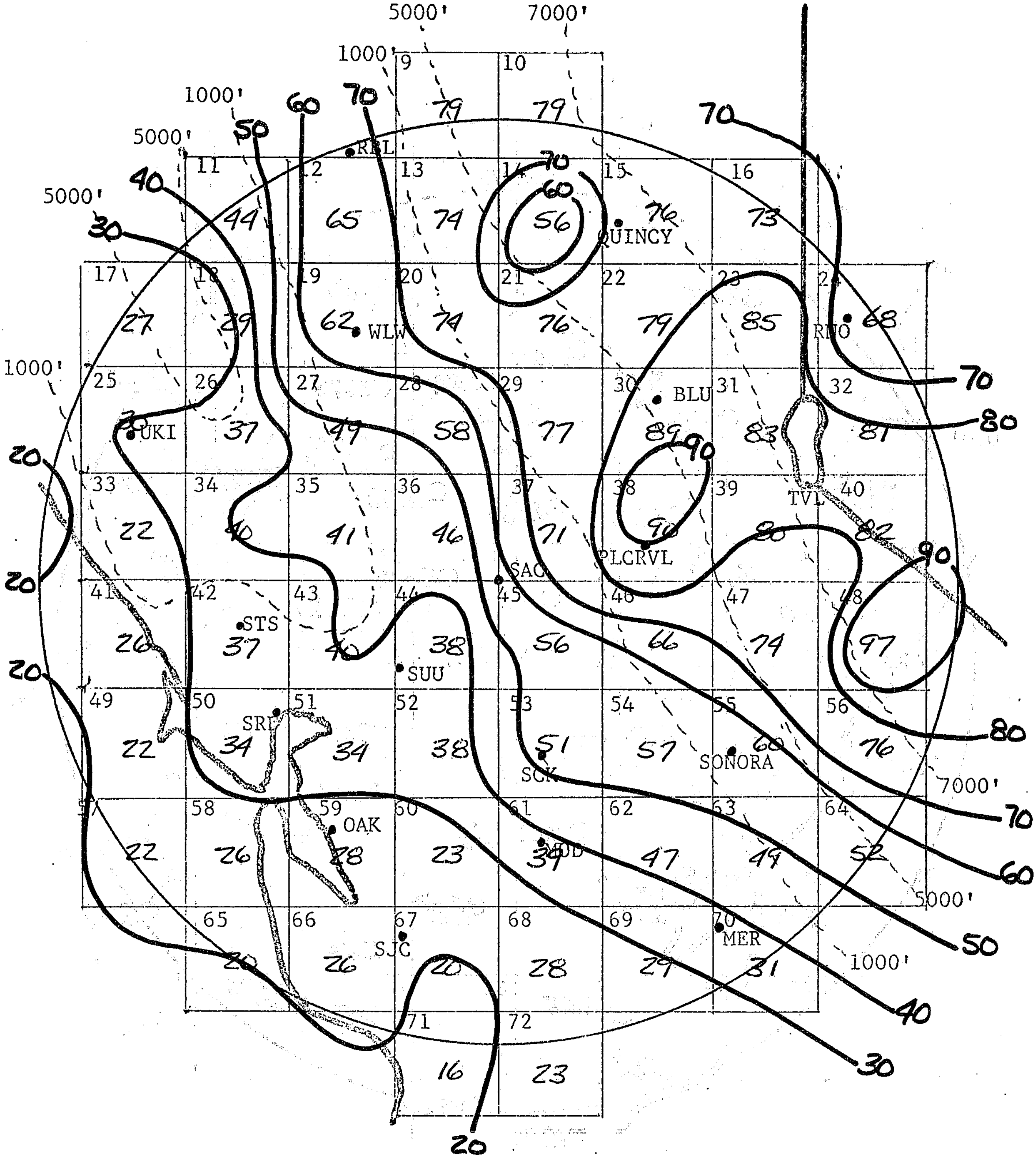

FIGURE 8. Average "dry" season (May-September) hourly echo frequencies. Dashed lines are approximate terrain contours. Grid numbers are in upper left corner of each square. Range circle is at 100 nautical miles.

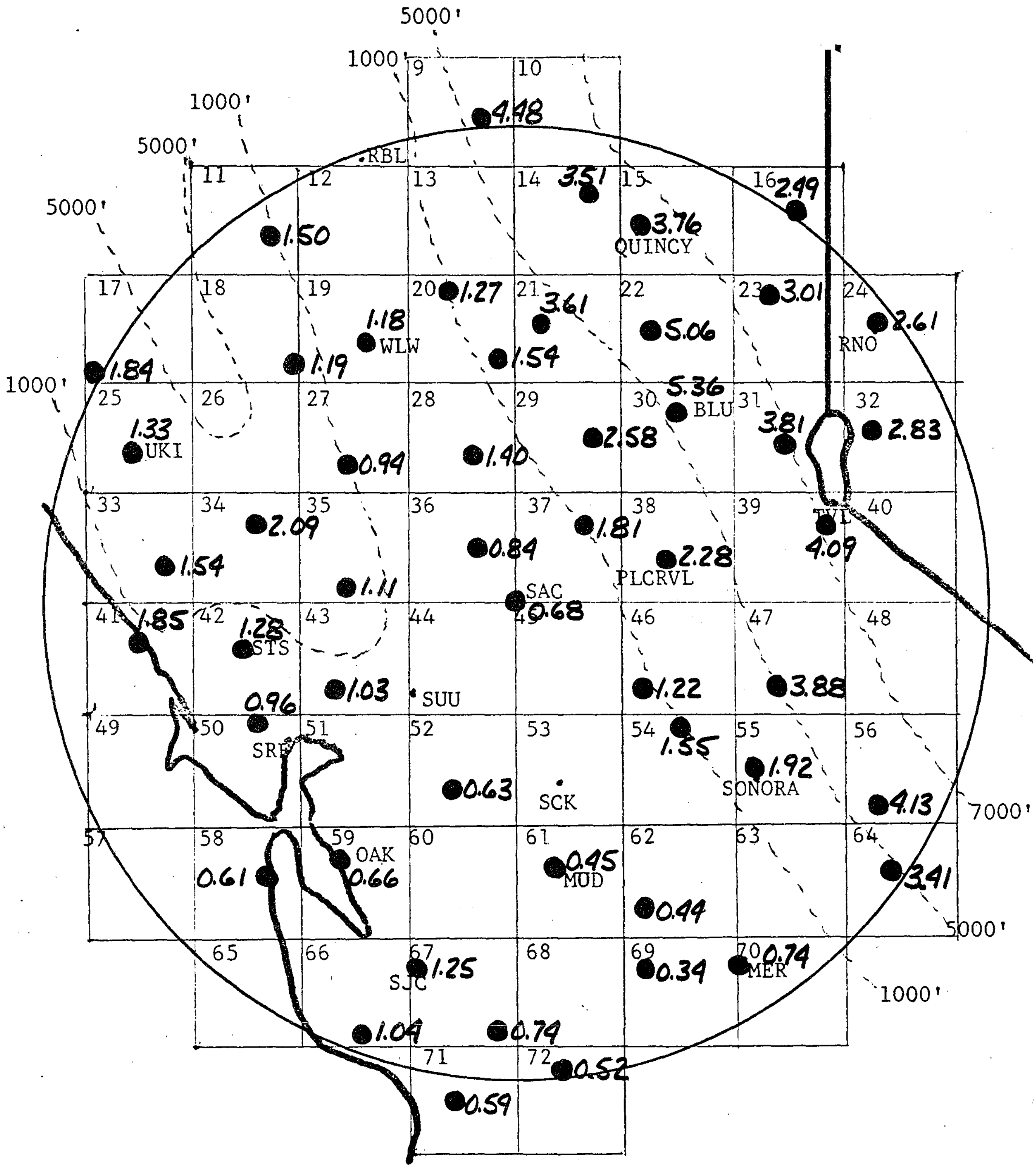

FIGURE 9. Average "dry" season gauge precipitation during period of radar record. See Table I in text for list of stations used. Dashed lines are approximate terrain contours. Grid numbers are in upper left corner of each square. Range circle is at 100 n.m.

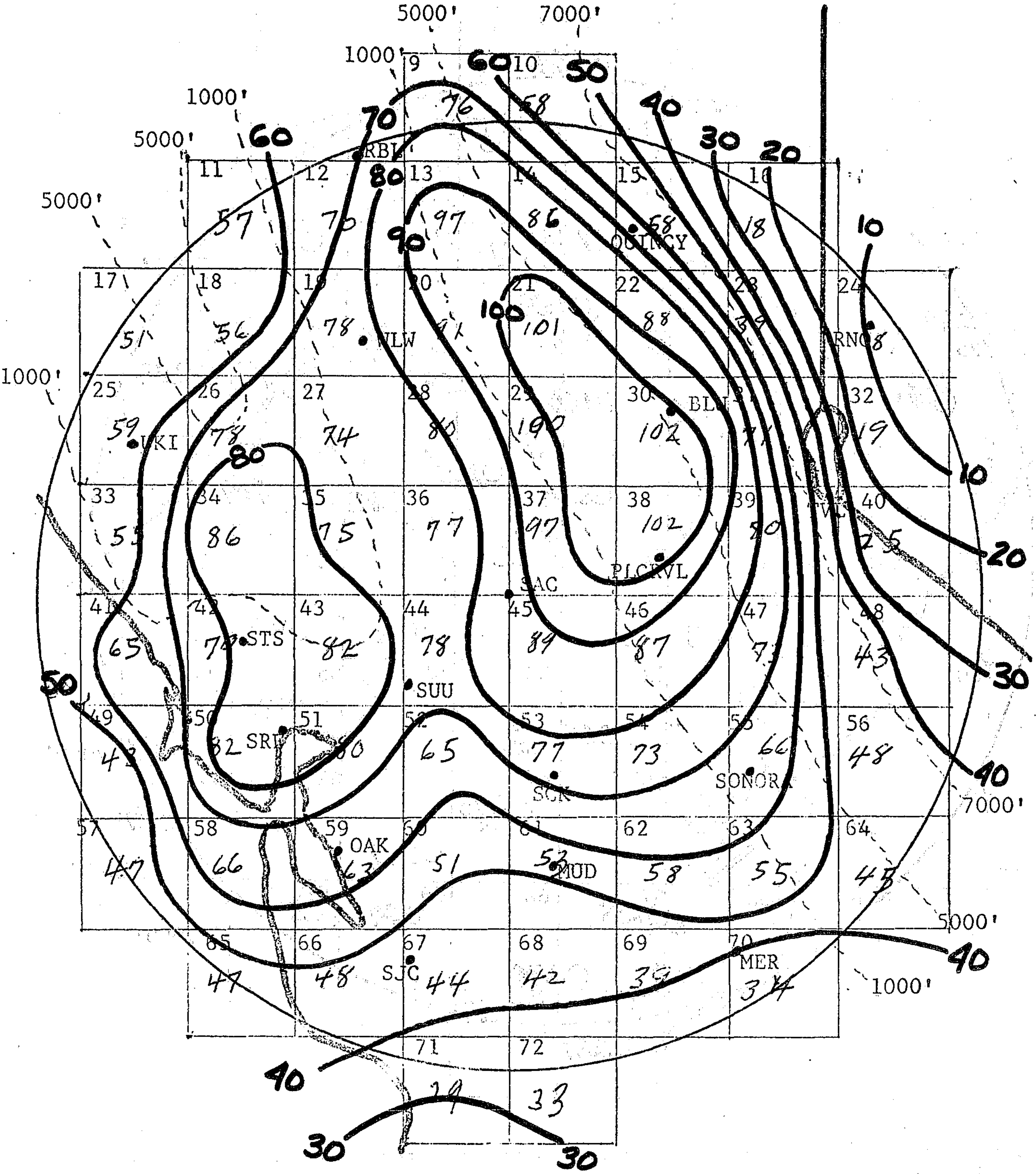

FIGURE 10. Average January Hourly echo frequencies. Dashed lines are approximate terrain contours. Grid numbers are in upper left corner of each square. Range circle is at 100 n.m.

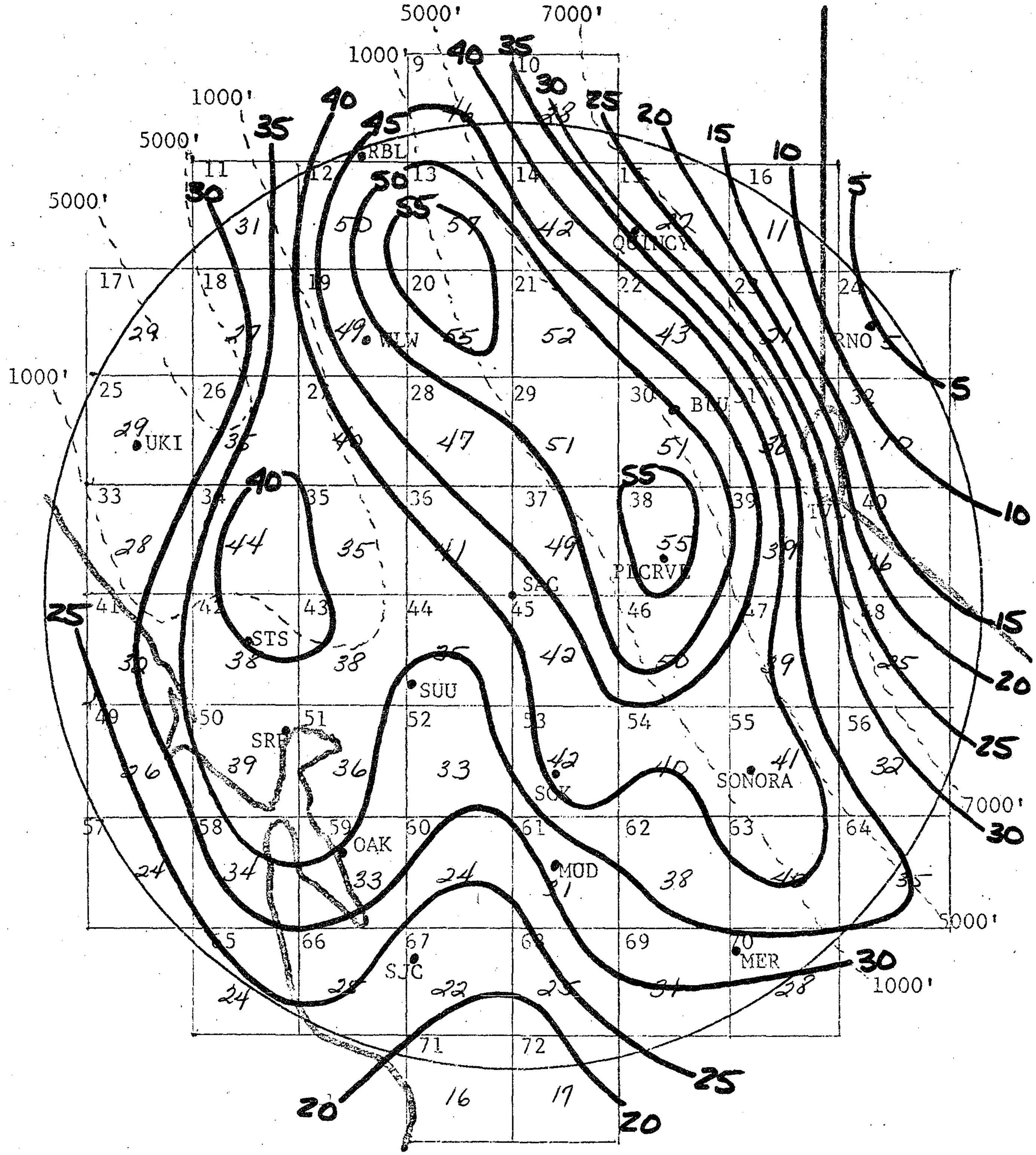

FIGURE 11. Average February hourly echo frequencies. Dashed lines are approximate terrain contours. Grid numbers are in upper left corner of each square. Range circle is at 100 n.m.

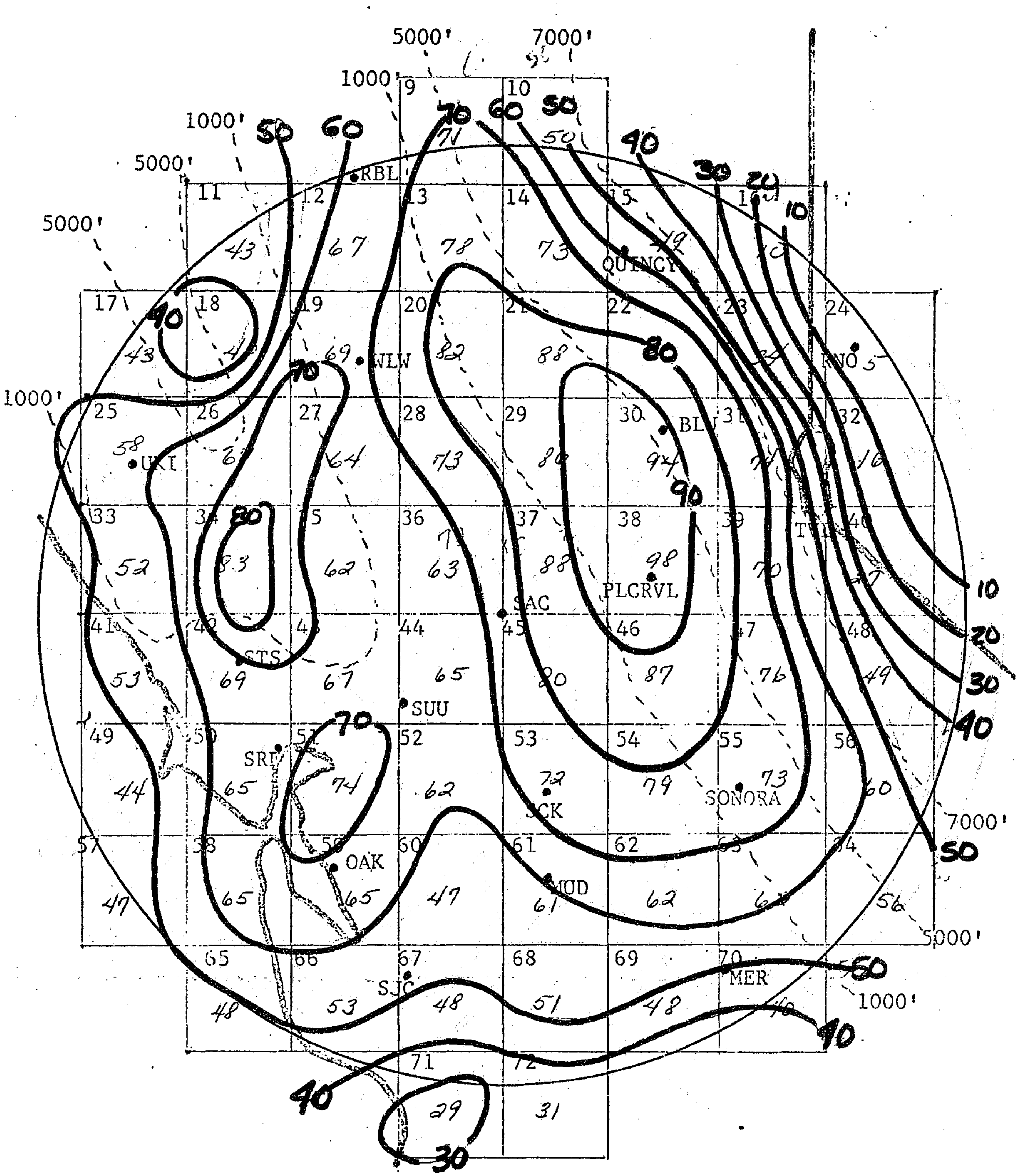

FIGURE 12. Average March hourly echo frequencies. Dashed lines are approximate terrain contours. Grid numbers are in upper left corner of each square. Range circle is at 100 n.m.

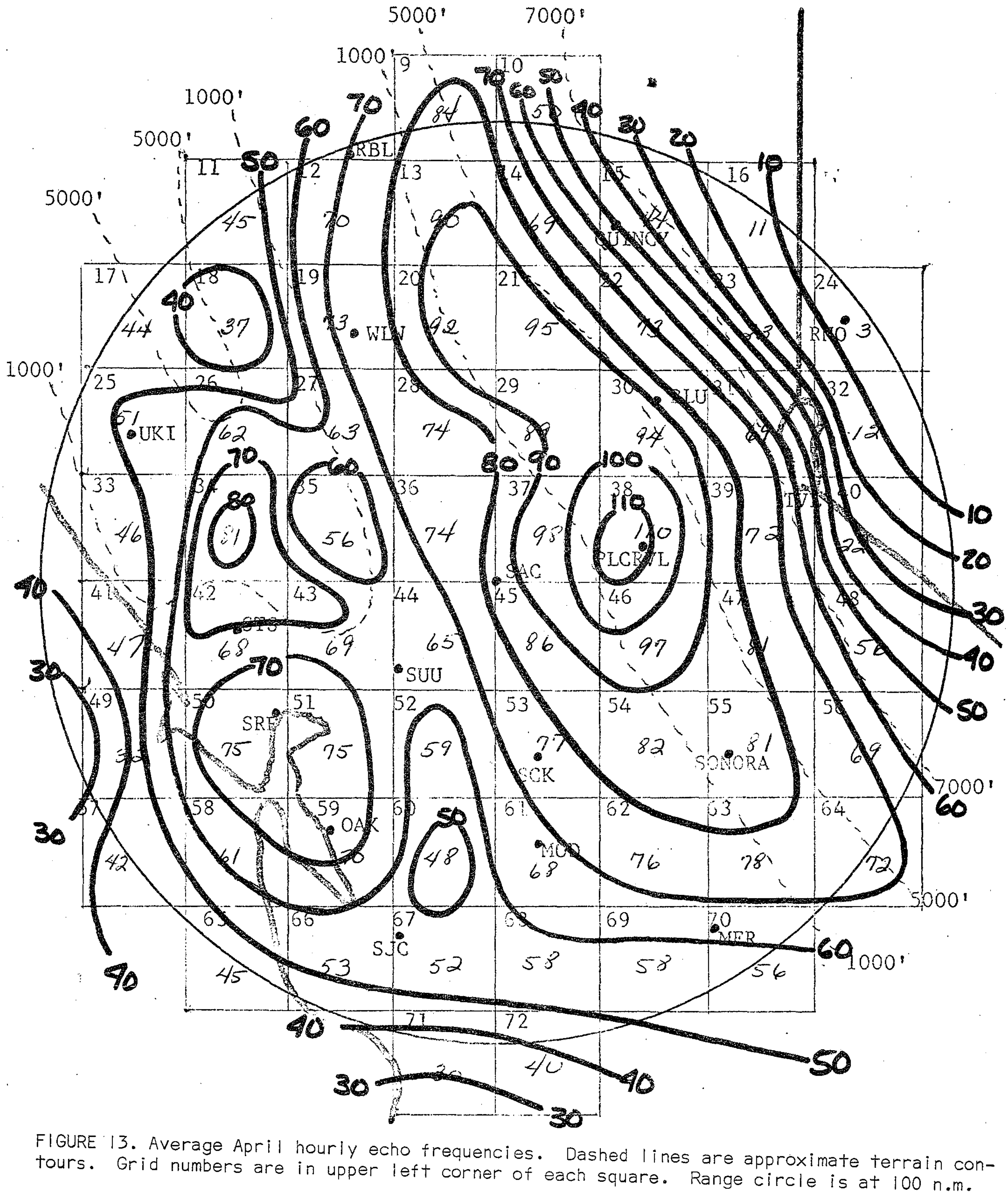

FIGURE 13. Average April hourly echo frequencies. Dashed lines are approximate terrain contours. Grid numbers are in upper left corner of each square. Range circle is at 100 n.m.

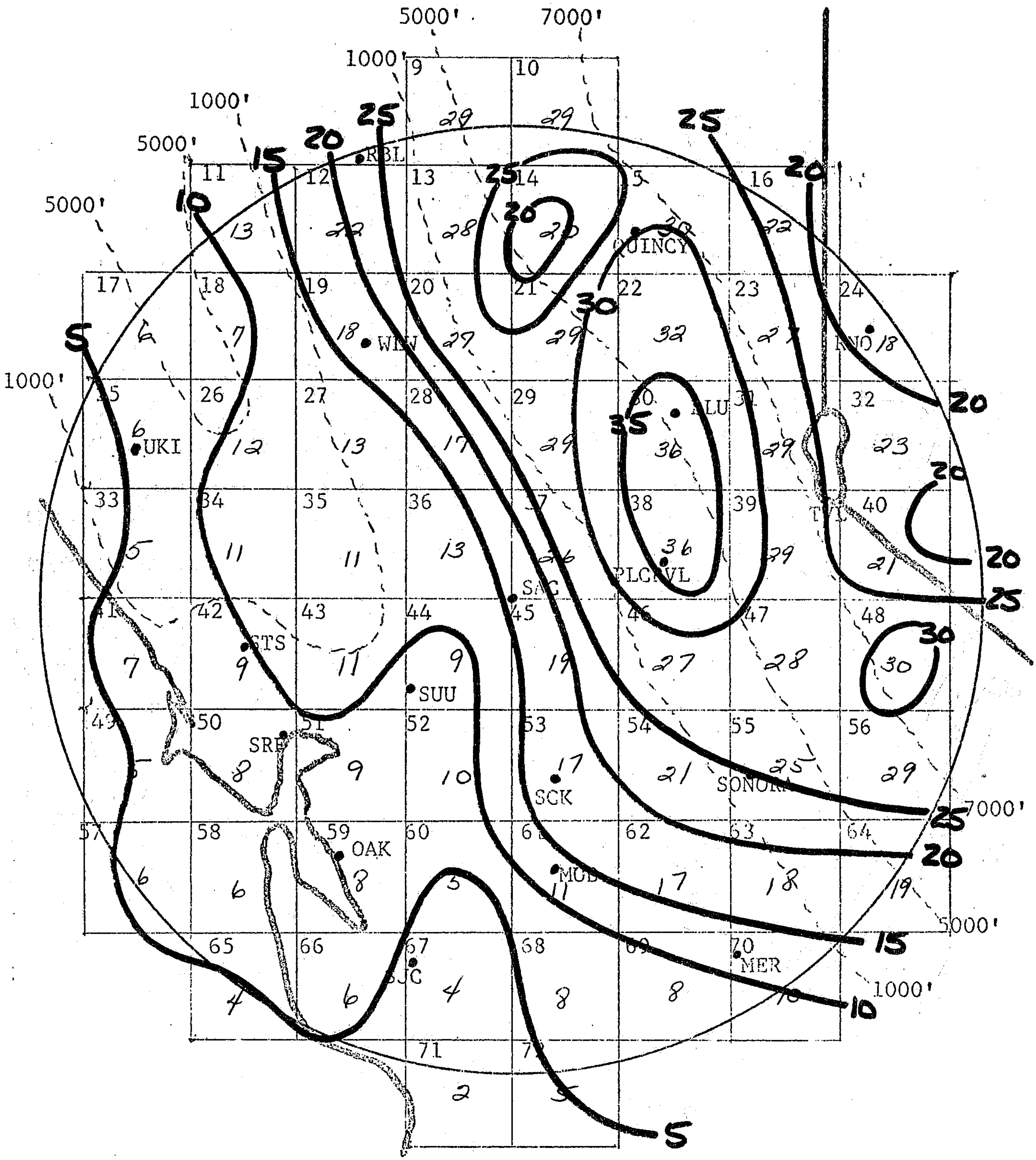

FIGURE 14. Average May hourly echo frequencies. Dashed lines are approximate terrain contours. Grid numbers are in upper left corner of each square. Range circle is at 100 n.m.

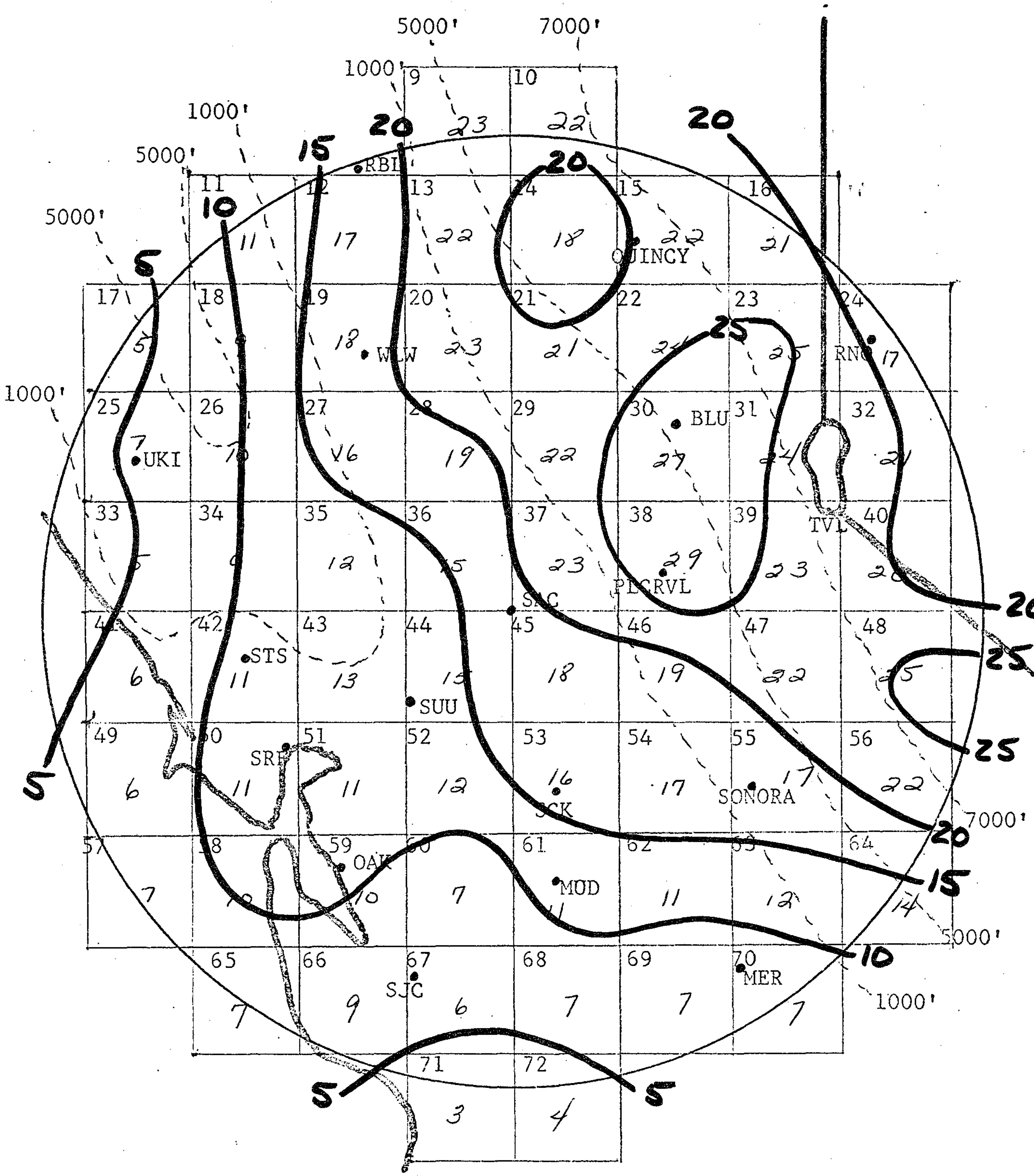

FIGURE 15. Average June hourly echo frequencies. Dashed lines are approximate terrain contours. Grid numbers are in upper left corner of each square. Range circle is at 100 n.m.

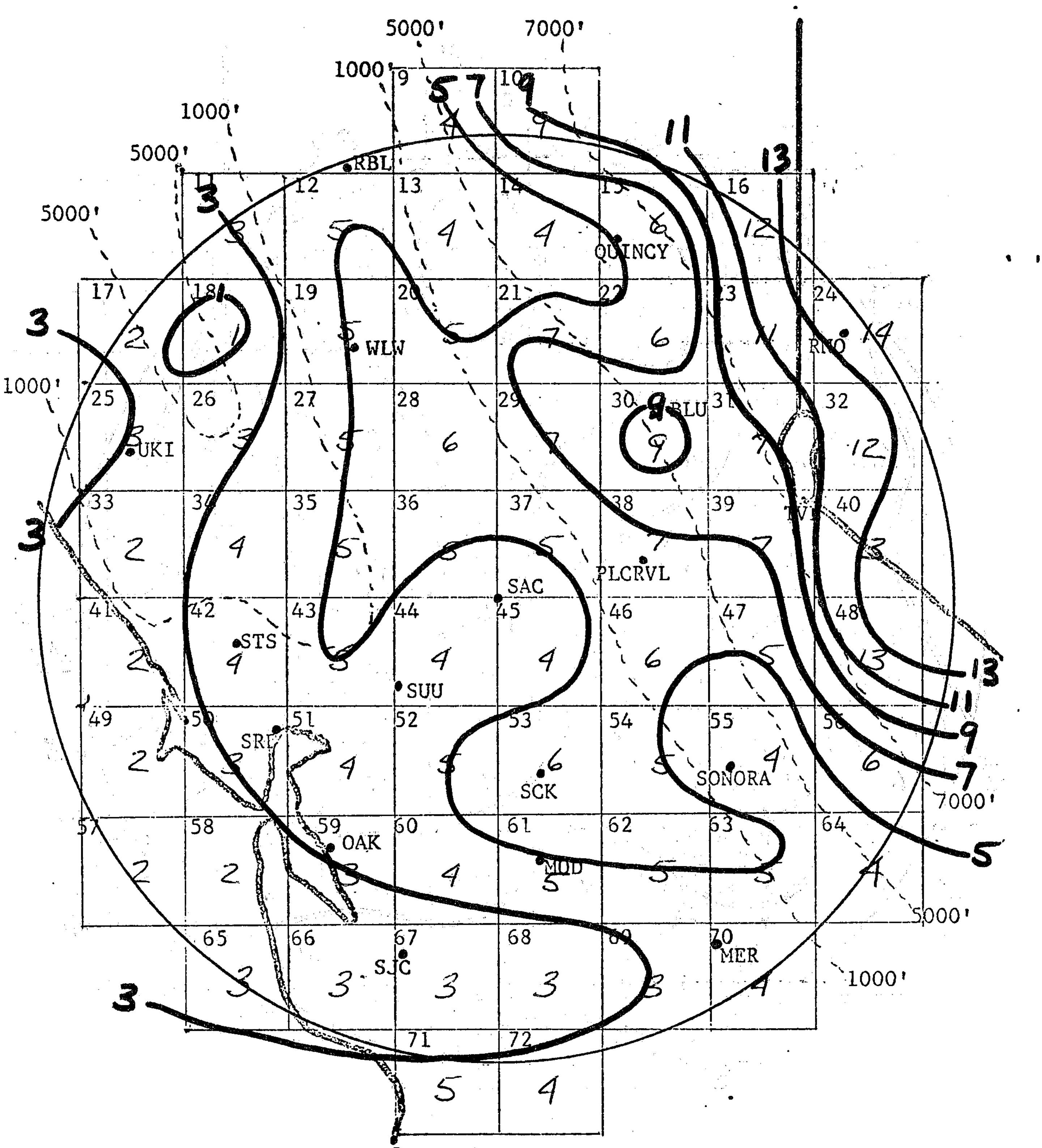

FIGURE 16. Average July hourly echo frequencies. Dashed lines are approximate terrain contours. Grid numbers are in upper left corner of each square. Range circle is at 100 n.m.

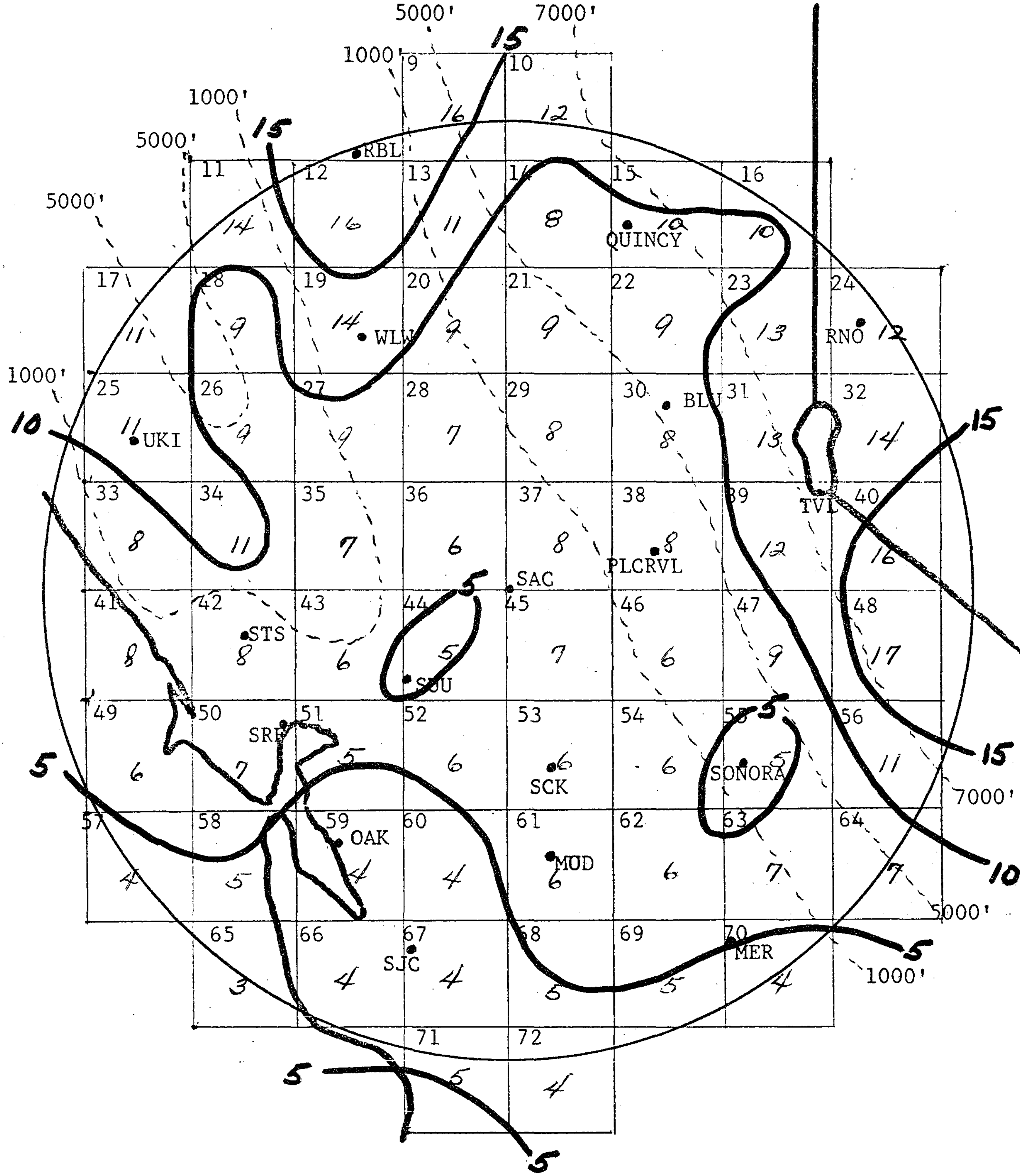

FIGURE 17. Average August hourly echo frequencies. Dashed lines are approximate terrain contours. Grid numbers are in upper left corner of each square. Range circle is at 100 n.m.

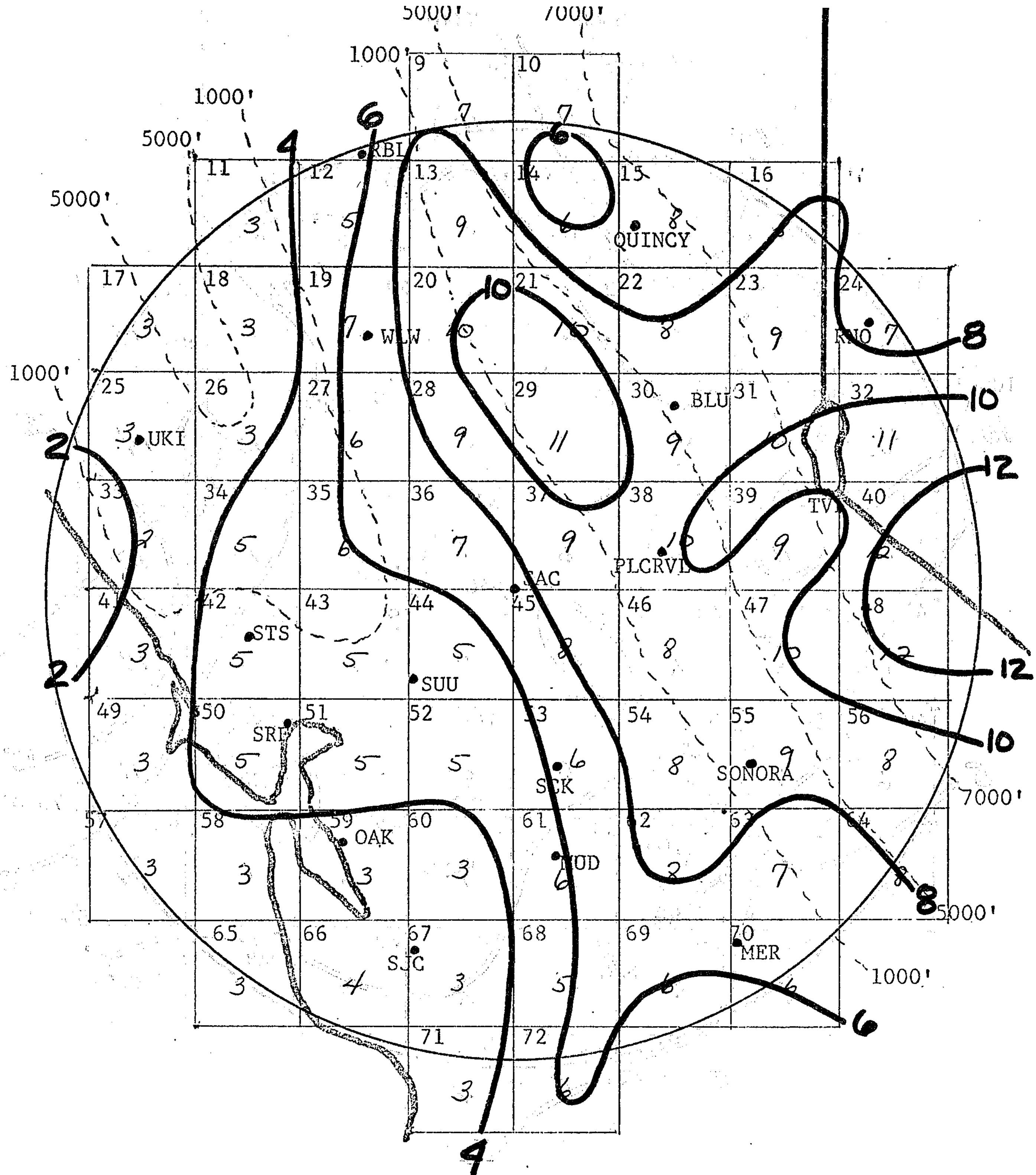

FIGURE 18. Average September hourly echo frequencies. Dashed lines are approximate terrain contours. Grid numbers are in upper left corner of each square. Range circle is at 100 n.m.

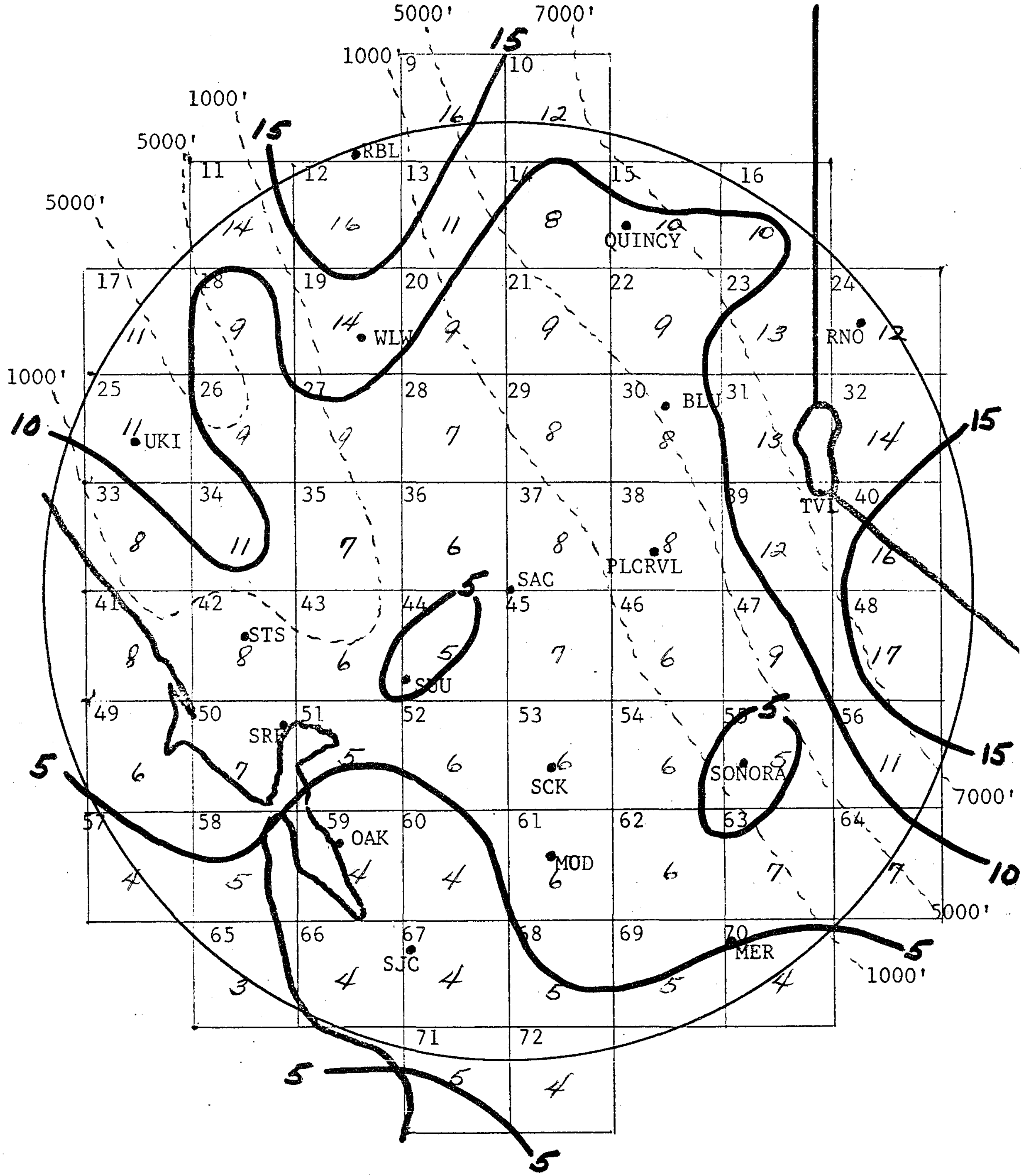

FIGURE 17. Average August hourly echo frequencies. Dashed lines are approximate terrain contours. Grid numbers are in upper left corner of each square. Range circle is at 100 n.m.

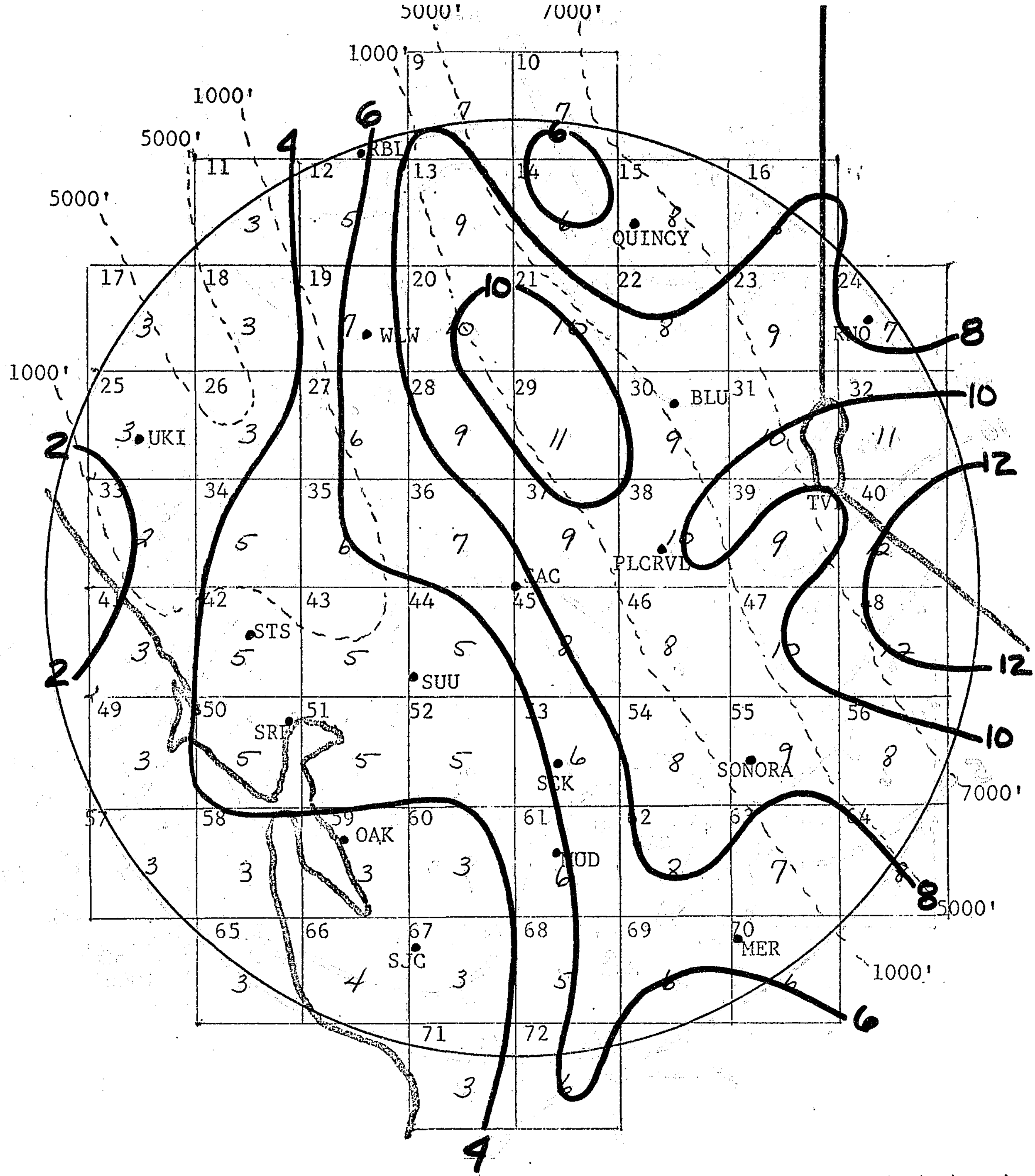

FIGURE 18. Average September hourly echo frequencies. Dashed lines are approximate terrain contours. Grid numbers are in upper left corner of each square. Range circle is at 100 n.m.

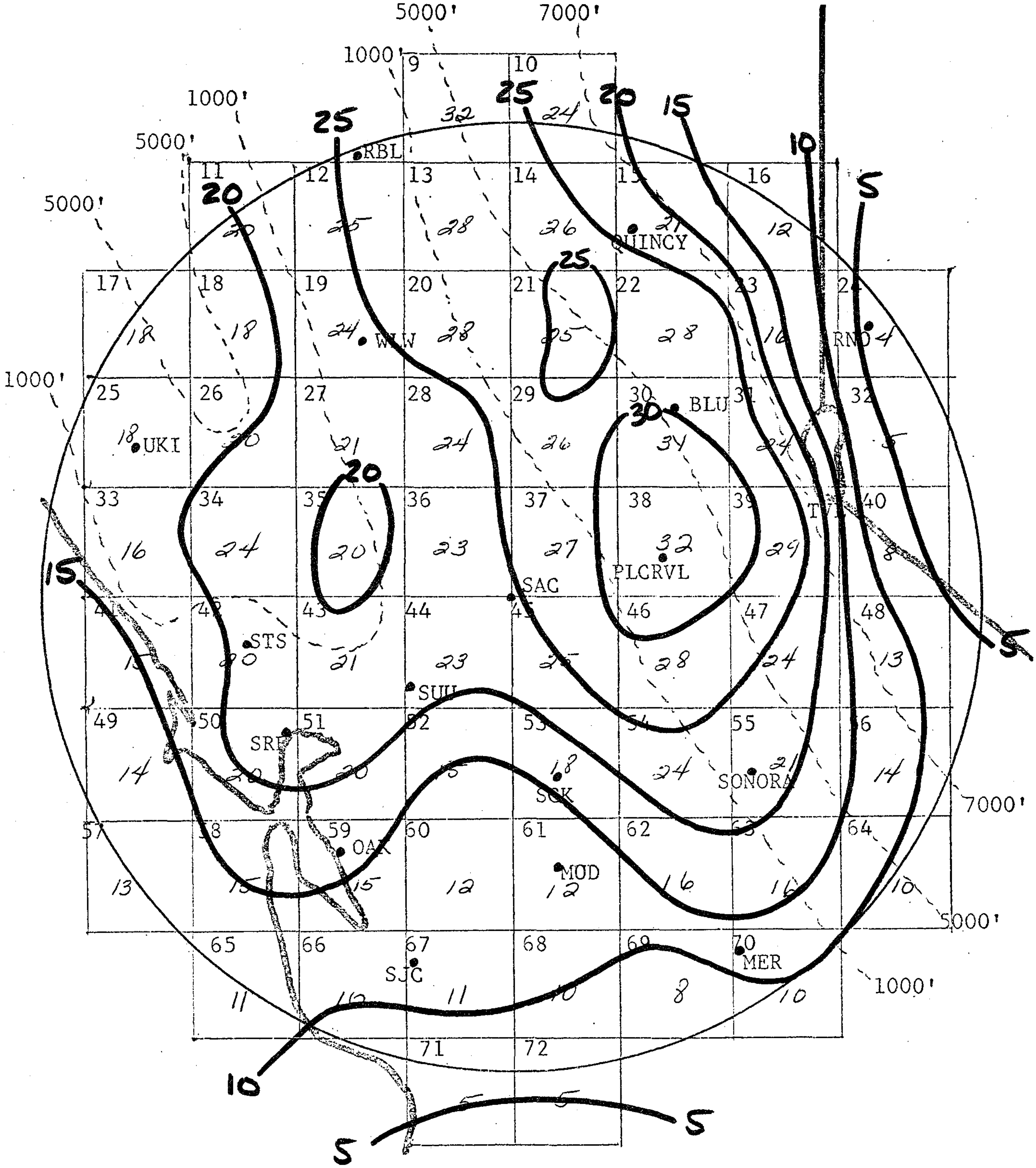

FIGURE 19. Average October hourly echo frequencies. Dashed lines are approximate terrain contours. Grid numbers are in upper left corner of each square. Range circle is at 100 n.m.

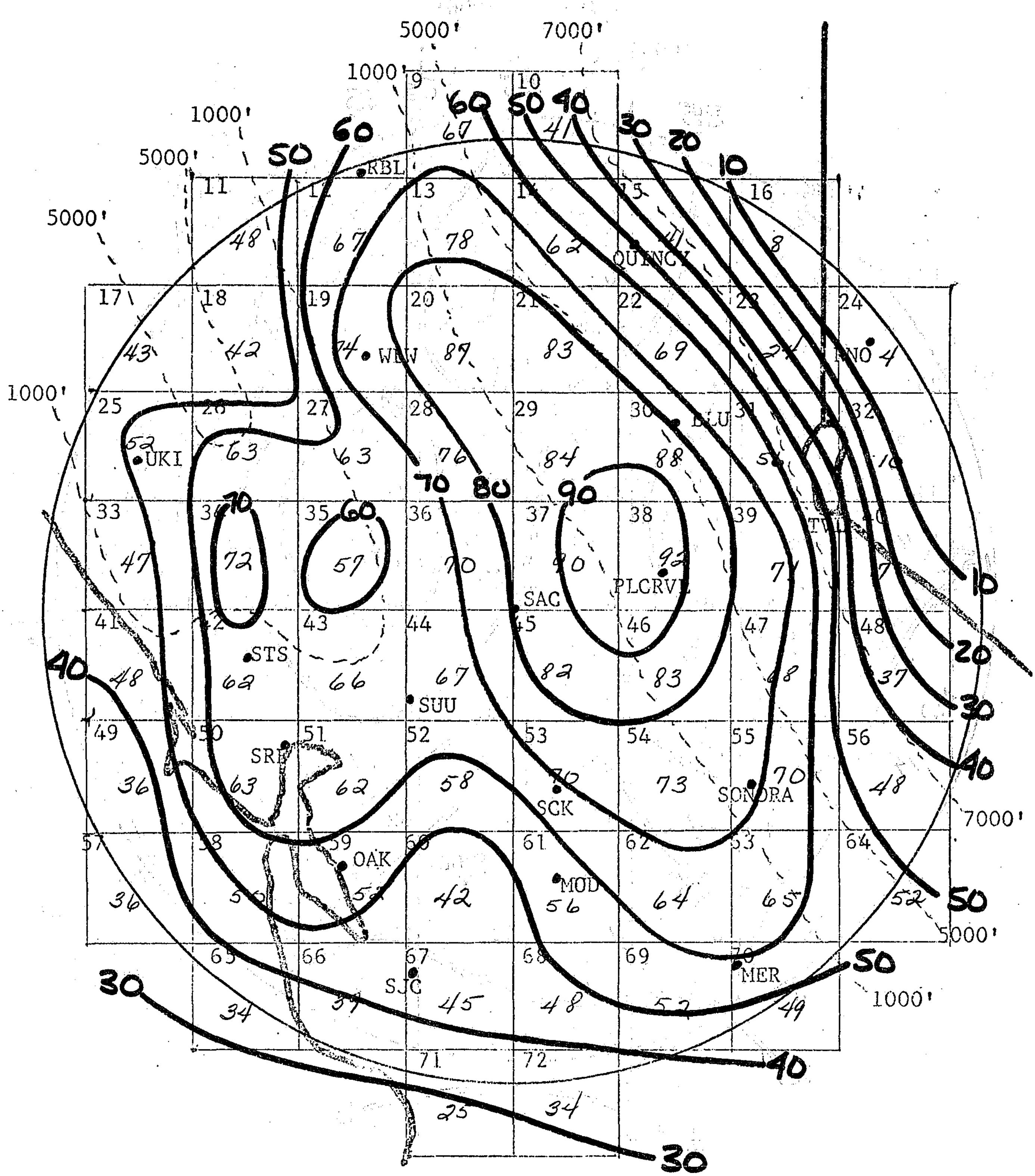

FIGURE 20. Average November hourly echo frequencies. Dashed lines are approximate terrain contours. Grid numbers are in upper left corner of each square. Range circle is at 100 n.m.

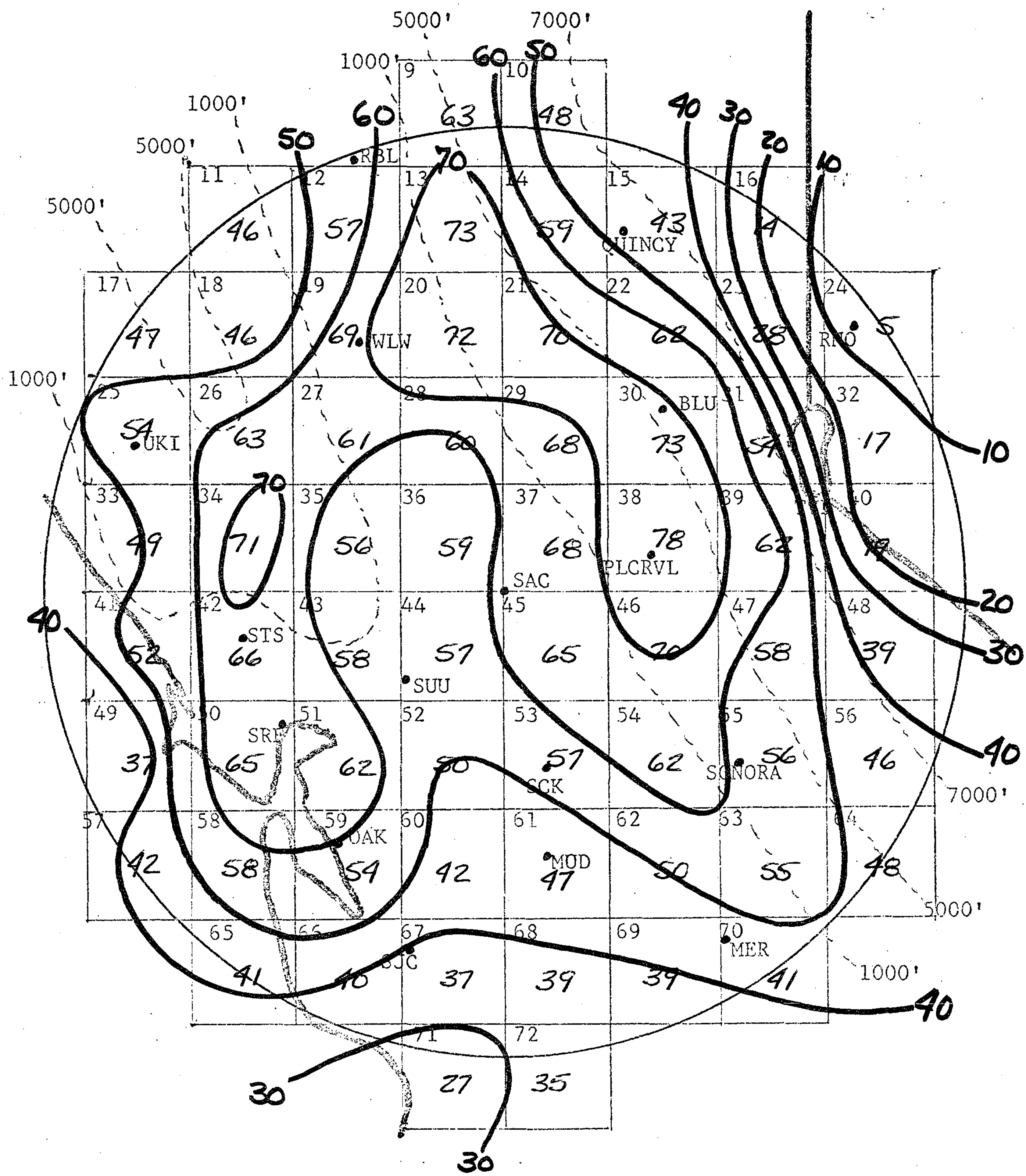

FIGURE 21. Average December hourly echo frequencies. Dashed lines are approximate terrain contours. Grid numbers are in upper left corner of each square. Range circle is at 100 n.m.

Western Region Technical Memoranda (Continued):

No. 27 Objective Minimum Temperature Forecasting for Helena, Montana. D. E. Olsen. February 1968. (PB-177 827)

No. 28** Weather Extremes. R. J. Schmidli. April 1968. (PB-178 928)

No. 29 Small-Scale Analysis and Prediction. Philip Williams, Jr. May 1968. (PB-178 425)

No. 30 Numerical Weather Prediction and Synoptic Meteorology. Capt. Thomas D. Murphy, U.S.A.F. May 1968. (AD-673 365)

No. 31* Precipitation Detection Probabilities by Salt Lake ARTC Radars. Robert K. Belesky. July 1968. (PB-179 084)

No. 32 Probability Forecasting in the Portland Fire Weather District. Harold S. Ayer. July 1968. (PB-179 289)

No. 33 Objective Forecasting. Philip Williams, Jr. August 1968. (AD-680 425)

No. 34 The WSR-57 Radar Program at Missoula, Montana. R. Granger. October 1968. (PB-180 292)

No. 35** Joint ESSA/FAA ARTC Radar Weather Surveillance Program. Herbert P. Benner and DeVon B. Smith. December 1968. (AD-681 857)

No. 36* Temperature Trends in Sacramento--Another Heat Island. Anthony D. Lentini. February 1969. (PB-183 055)

No. 37 Disposal of Logging Residues Without Damage to Air Quality. Owen P. Cramer. March 1969. (PB-183 057)

No. 38 Climate of Phoenix, Arizona. R. J. Schmidli, P. C. Kangieser, and R. S. Ingram. April 1969. (PB-184 295)

No. 39 Upper-Air Lows Over Northwestern United States. A. L. Jacobson. April 1969. (PB-184 296)

No. 40 The Man-Machine Mix in Applied Weather Forecasting in the 1970s. L. W. Snellman. August 1969. (PB-185 068)

No. 41 High Resolution Radiosonde Observations. W. W. Johnson. August 1969. (PB-185 673)

No. 42 Analysis of the Southern California Santa Ana of January 15-17, 1966. Barry B. Aronovitch. August 1969. (PB-185 670)

No. 43 Forecasting Maximum Temperatures at Helena, Montana. David E. Olsen. October 1969. (PB-187 762)

No. 44 Estimated Return Periods for Short-Duration Precipitation in Arizona. Paul C. Kangieser. October 1969. (PB-187 763)

No. 45/1 Precipitation Probabilities in the Western Region Associated with Winter 500-mb Map Types. Richard P. Augulis. Dec. 1969. (PB-188 248)

No. 45/2 Precipitation Probabilities in the Western Region Associated with Spring 500-mb Map Types. Richard P. Augulis. Jan. 1970. (PB-184 434)

No. 45/3 Precipitation Probabilities in the Western Region Associated with Summer 500-mb Map Types. Richard P. Augulis. Jan. 1970. (PB-189 414)

No. 45/4 Precipitation Probabilities in the Western Region Associated with Fall 500-mb Map Types. Richard P. Augulis. Jan. 1970. (PB-189 435)

No. 46 Applications of the Net Radiometer to Short-Range Fog and Stratus Forecasting at Eugene, Oregon. L. Yee and E. Bates. Dec. 1969. (PB-190 476)

No. 47 Statistical Analysis as a Flood Routing Tool. Robert J. C. Burnash. December 1969. (PB-188 744)

No. 48 Tsunami. Richard P. Augulis. February 1970. (PB-190 157)

No. 49 Predicting Precipitation Type. Robert J. C. Burnash and Floyd E. Hug. March 1970. (PB-190 962)

No. 50 Statistical Report of Aeroallergens (Pollens and Molds) Fort Huachuca, Arizona 1969. Wayne S. Johnson. April 1970. (PB-191 743)

No. 51 Western Region Sea State and Surf Forecaster's Manual. Gordon C. Shields and Gerald B. Burdwell. July 1970.

*Out of Print
**Revised